

## 4 GEOTECHNICAL ASPECTS ON THE SOUTH ISLAND OF NEW ZEALAND

This chapter identifies locations of liquefaction manifestations and discusses the effects of liquefaction and related phenomena on the South Island of New Zealand resulting from the 2016,  $M_w$ 7.8 Kaikoura earthquake. Detailed observations are recorded to document the occurrence and non-occurrence of liquefaction in areas shaken at different levels of intensity. Strong motion recordings indicate high peak ground accelerations (PGA) occurred in the Waiiau valley of North Canterbury (marked “Area C” in Figure 4.1). Horizontal accelerations at the Waiiau strong motion station (WTMC) were in excess of 1 g and vertical accelerations in excess of 2.7 g. The ground motions were significantly attenuated in the main urban areas of the South Island; the recorded peak ground accelerations were in the range of 0.14 g to 0.27 g in the areas around Blenheim (Area A) and Kaikoura (Area B). A more detailed summary of the ground motion characteristics across the South Island is provided in Chapter 3 of this report.

In the days and weeks following the earthquake, a collaborative approach was taken to the reconnaissance across the South Island, and involved New Zealand researchers and engineers, as well as visiting academics and members of the Geotechnical Extreme Events Reconnaissance (GEER). Association. Reconnaissance was undertaken in 3 phases. In the days following the earthquake, exploratory missions were undertaken to define broad areas where earthquake-related damage had occurred. Additional field surveys were undertaken in the areas marked A to C in Figure 4.1 between 17<sup>th</sup> November and 11<sup>th</sup> December 2016 first to record perishable data (such as evidence of liquefaction, lateral spreading, and damage to structures) and later to characterise specific sites.

Given the geographic distribution of the varying geologic settings, liquefaction hazard, and ground motions, each of the four areas shown in Figure 4.1 are presented separately in subsequent sections of this chapter in order of north to south. In the area of Blenheim, severe liquefaction and lateral spreading occurred on the flood plains of the Wairau River, particularly on inner meander bends and locations of paleo features. In Kaikoura, a series of localised failures in soft soil deposits caused large lateral displacements along Lyell Creek and caused damage to a number of houses built within 30 m of the creek. Despite the extreme ground motions recorded close to the town of Waiiau, relatively little evidence of liquefaction was observed, and the main impacts in this area were to the bridges, many of which showed severe structural distress. Detailed reconnaissance in Christchurch (Area D) was not carried out, though observations from four sites in the city and towns to the north are briefly discussed.

It is important to state that while a number of examples of damage are presented in this paper, the most significant impacts of the 2016 Kaikoura Earthquake arose from the numerous landslides across the South Island (which cut off the town of Kaikoura, as well as blocking and severely damaging the N-S highway and railway). These aspects are outside the scope of this report.

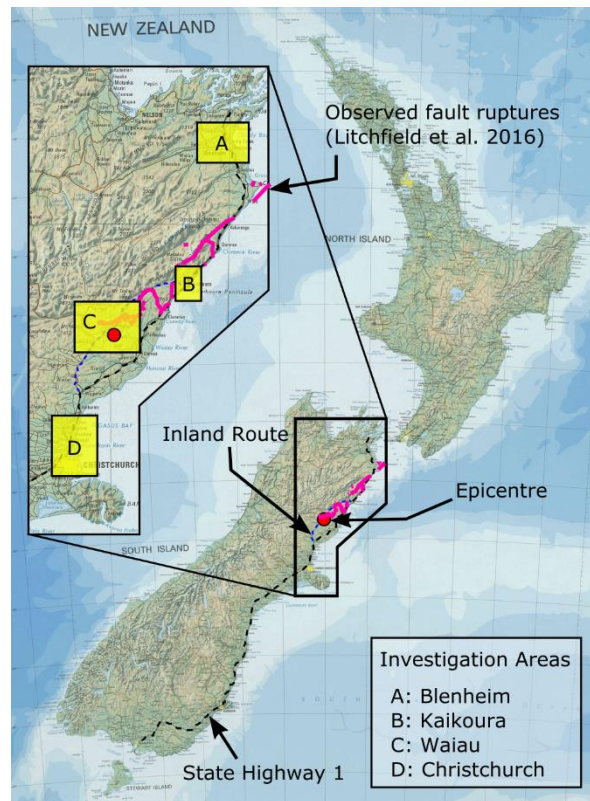


Figure 4.1: Location of main reconnaissance areas. Dashed lines indicate road routes outside of these main areas that were also surveyed by reconnaissance teams.

#### 4.1 Summary of Reconnaissance - Marlborough

The region of Marlborough is located at the north-eastern corner of the South Island, New Zealand. The landscape is dominated by a series of north-east trending mountain ranges and intervening valleys associated with uplift along the major faults within the Marlborough Fault Zone. The region has a high level of seismic hazard due to the many active faults within the region, including the Wairau, Clarence, Awatere, Kekerengu and Vernon faults (Begg & Johnston, 2000). The township of Blenheim is situated approximately 5 km from the east coast, within the relatively flat expanse of the Wairau Plain within the Wairau Valley. It has a population of ~30,700 and a total urban area of approximately 104 km<sup>2</sup>, resulting in a relatively low urban density of ~300 people/km<sup>2</sup>.

The Wairau Valley is transected by the braided Wairau River which flows eastwards approximately along the trace of the Wairau Fault. The township is predominantly situated upon Holocene swamp deposits composed of poorly consolidated silt, mud, peat, and sand. To the west, alluvial outwash gravels deposited by the Wairau River predominate while Holocene coastal and marine sands to silts predominate to the east and are locally cross-cut by young fluvial sands to silts. The coastal sediments reflect marine regression and coastal progradation following the mid-Holocene highstand with the coastline approximately extending inland to the eastern extent of the township at approximately 6,500 years before present. The interaction of the alluvial and marine processes proximal to the coast likely resulted in the swamp formed within the township.



Figure 4.2: Overview of the Marlborough region and location of significant historic earthquakes.

Sediments within the township have been re-worked and re-deposited by the Wairau River and meandering Opaoa and Taylor Rivers within the township. The rivers within the region have been extensively modified to improve drainage and reduce flooding within the township. The Opaoa River is fed from the Omaka River and was re-named from the Opawa River in 2015, as a result, the previous spelling is present in historical maps of the region. The loosely consolidated fine sands to silts deposited by these rivers, combined with high water table levels (1-2 m) to the east of the township pose a localized high liquefaction hazard.

The Marlborough region has experienced liquefaction in previous historic earthquakes, namely the 1848 Marlborough earthquake, the 1855 Wairarapa earthquake, and minor episodes during the 2013 Cook Strait earthquake sequence (epicentres of these earthquakes are summarised in Figure 4.2). Written accounts from the Mw7.5 1848 Marlborough earthquake (Mason & Little 2006) suggest the occurrence of lateral spreading, sand ejecta and subsidence in the Wairau Plain (Arnold 1847):

*“the effects of the earthquake were very apparent on the river bank: there were a great many large cracks in the ground, some as much as two feet wide: and I also saw numerous deep holes, by which a lower stratum of sand and water had burst its way thro' the overlying ground, and covered everything with sand for some distance.”*

The Mw8.2 Wairarapa earthquake again resulted in liquefaction surface manifestations across the Wairau Plain, and in the Awatere and Clarence Valleys along the rivers. A basic summary of the

areas affected is presented in Figure 4.3; Thompson (1859) provides an example of a written account from the time:

*“in the Wairau Valley ... near the river bed, numerous systems of earthquake fissures can be observed, which always trend parallel to the course of the river and are intersected at various angles by abrupt bends in the river” and that “several fissures in the earth, four feet deep, and sufficient to admit a man, yawned....”*

Another significant event in this region was the  $M_w$ 5.8 1966 Seddon earthquake. Structural and infrastructure damage occurred during this event. No evidence of liquefaction was reported, but it is possible minor liquefaction occurred in rural areas and went unreported.

During the 2013 Cook Strait earthquake sequence there was evidence of minor liquefaction manifestation following the 16 August 2013  $M_w$ 6.6 Lake Grassmere earthquake. This damage was confined to the highly susceptible sediments to the east of Blenheim (mainly along the Opaoa River) and in the Awatere Valley region, including damage on the southern edge of Lake Grassmere close to the epicentre of the earthquake, at the approaches of the Awatere Bridge and a number of other smaller bridges in the region.

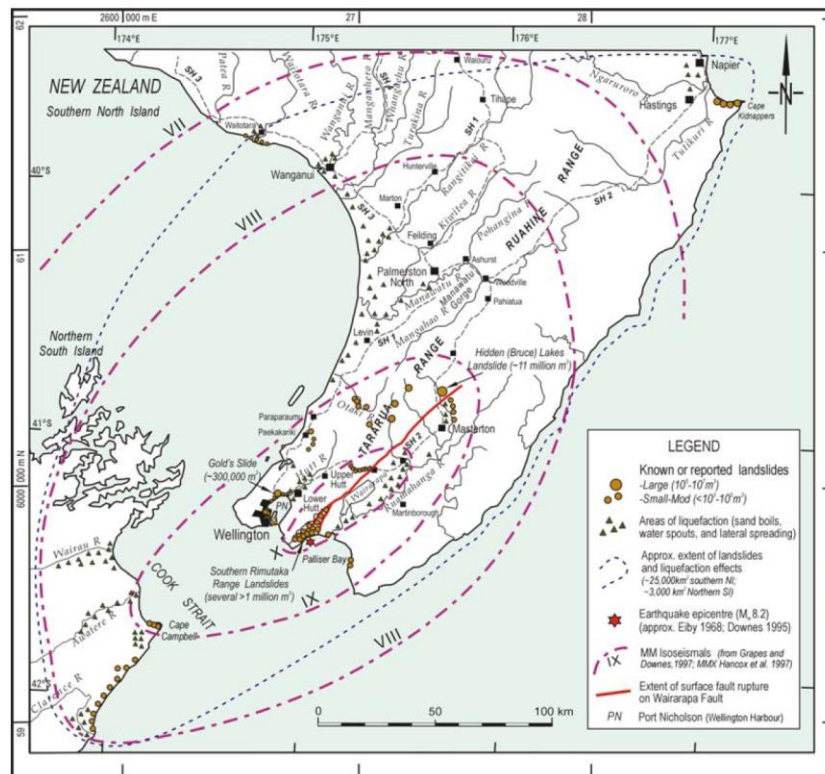


Figure 4.3: Map showing location of known landsliding and manifestation of liquefaction due to the 1855 Wairarapa earthquake (after Hancox 1997). The Marlborough region is in the lower left corner of this figure.

The reconnaissance in the Marlborough region focussed on the outlined area in Figure 4.4. There were two sets of reconnaissance surveys undertaken in this region, the initial survey was conducted between 17 and 18 November 2016 and a follow up survey was conducted between 5 and 7 December 2016. The information collated during these surveys was complemented by information gathered from local consulting engineers and the Marlborough District Council.

Within the Wairau valley, liquefaction and lateral spreading was the major feature of ground damage, and was largely observed along the Lower Wairau and Opaoa Rivers. Severe manifestations of liquefaction were recorded in the area of the Equestrian Park and the Blenheim Rowing Club. However, very few buildings are present in these areas, and the engineering impact was generally low. It is also important to note that despite the very loose nature of these deposits, the extent and quantity of ejecta is significantly less than what was observed in either of the 2010 Darfield or 2011 Christchurch Earthquakes (Cubrinovski et al. 2010, Cubrinovski et al. 2011). Some moderate liquefaction was observed in a few locations within the township of Blenheim, but these locations were either along the river or in the area of the sports fields at the north of the town and had limited impact on infrastructure.

The first part of this chapter focusses on the damage within the urban extents of Blenheim and particular sites of interest in the area. The second part of this chapter focusses on damage along the rivers outside of Blenheim within the Wairau Plains.

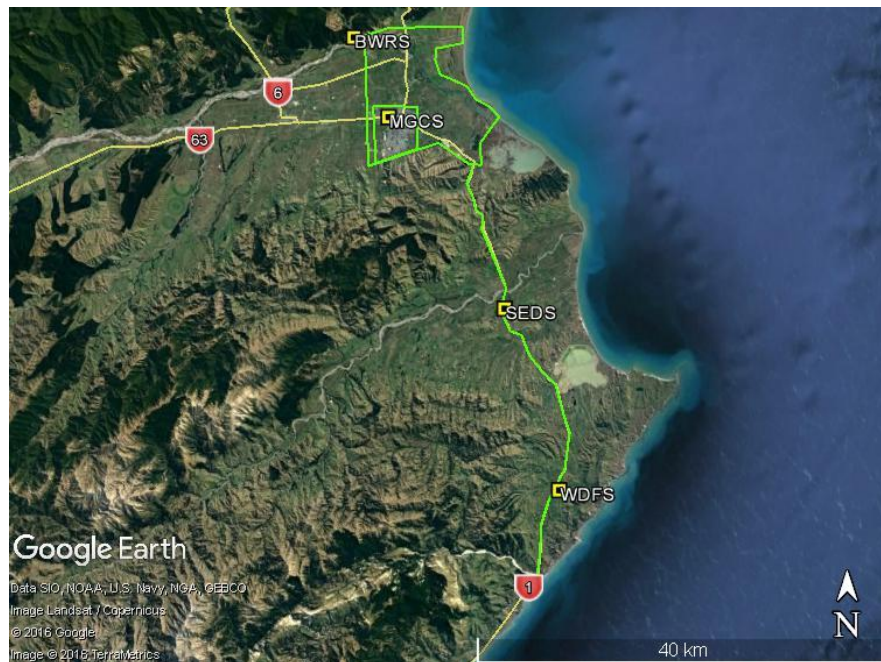


Figure 4.4: Overview map of reconnaissance areas in Marlborough outlined in green and path along State Highway 1. Location of strong motion stations highlighted in this figure, with MGCS in the Blenheim Urban Area.

The ground motion intensity varied significantly over the Marlborough region, with the location of the strong motion stations shown in Figure 4.4. In Ward, the station WDFS recorded a geometric mean horizontal PGA of approximately 1.1 g. Further to the north in Seddon a geometric mean PGA = 0.66 g was obtained (station SEDS), and the shaking was PGA = 0.22 g (station MGCS) in the Blenheim (i.e. Lower Wairau River area).

#### 4.1.1 Blenheim Urban Area

Both reconnaissance surveys and discussions with local engineers and Marlborough District Council were able to provide a detailed summary of the liquefaction related impacts and manifestations in the Blenheim urban area. Figure 4.5 summarises these locations, with all other areas not affected by liquefaction surface manifestations. Localized evidence of lateral spreading and liquefaction ejecta were observed within the inner meander bends of the Taylor River and Opaoa Rivers within this area. No evidence of lateral spreading was observed within the outer meander bends, nor beneath any of the road bridges surveyed.

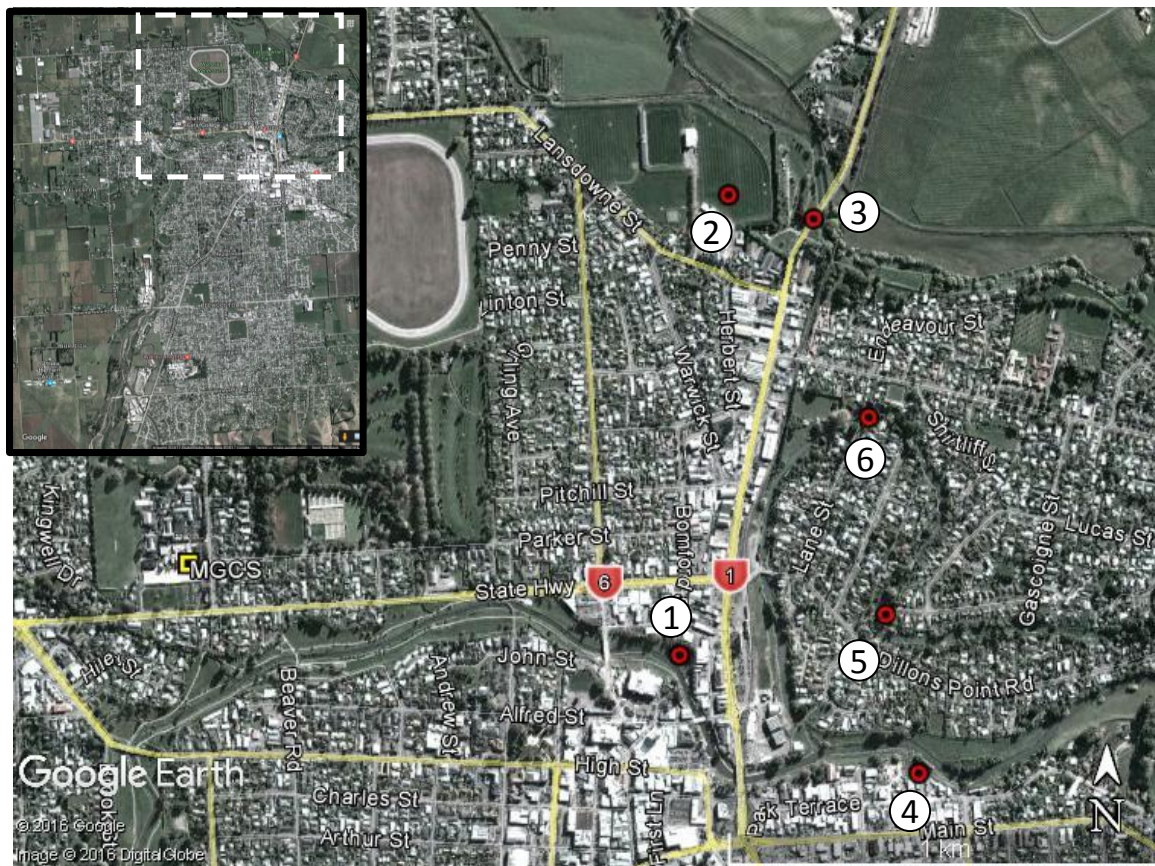


Figure 4.5: Map summarising impacts in urban Blenheim, and location of the MGCS SMS. Inset indicates area where all liquefaction impacts have been summarised and the zoomed in area highlighted in the wider figure (approx. centre of image: S41.5046, E173.9545).

#### 4.1.1.1 Taylor River

Localized cracking and elliptical liquefaction ejecta features were observed along the northern bank of the Taylor River, in the area behind 3-7 Auckland Street (Location 1 in Figure 4.5). This area was less than a metre above the river level and was relatively flat as shown in Figure 4.6. The ejecta were observed in a depression that was filled with standing water and located approximately 10 m away from river bank. The ejecta feature ranges in length from 5 to 7 m, and 1 to 1.2 m in diameter (Figure 4.6). Cracks approximately 2 to 5 cm wide were observed in a garden, also located within the depression, and were surrounded by localized liquefaction ejecta. The ejecta were uniformly composed of grey fine-medium sand and the particle size distributions of these ejecta are shown in Figure 4.7 (marked in the legend as TR-1 and TR-2). No ejecta or cracking was observed within 10 m of the river bank. The area was formerly within the meandering channel of the Taylor River before modification and straightening of the river took place in 1969, subsequently reducing flow levels (Marlborough District Council 2017). No other evidence of liquefaction manifestation was observed upstream of this point along the Taylor River.



Figure 4.6: Localized elliptical liquefaction ejecta features along the northern bank of the Taylor River (Location 1 in Figure 4.5), approximately 10 to 15 m from the river (S41.5096, E173.9577, facing SE).

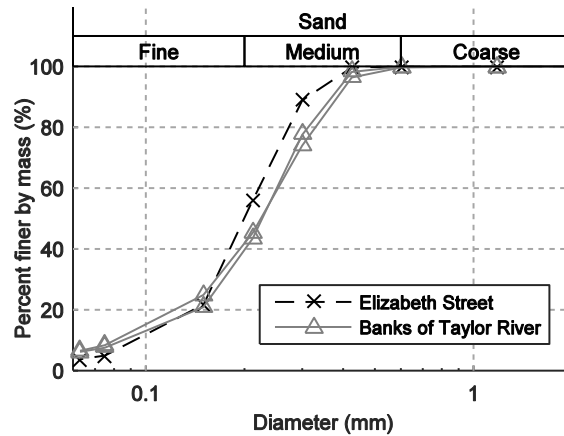


Figure 4.7: Particle size distribution of ejecta samples in the Blenheim CBD area (Taylor River: TR-1 & TR-2 (S41.5095, E173.9575) and Elizabeth Street: EC-1 (S41.5089, E173.9636)).

#### 4.1.1.2 Lansdowne Park

Surficial evidence of liquefaction was observed in the area of Lansdowne Park on the northern edge of Blenheim (Location 2 in Figure 4.5). The main sports facility was built in the area south of the current channel of the Opaoa River. The locations of ejecta in the southern area of the park were surveyed by local engineers and are shown superimposed on aerial photography in Figure 4.8. Additionally, the location where ejecta samples were collected are designated with blue stars. It should be noted that additional liquefaction features formed to the north of the rugby pitch which are not shown.

Cone penetration tests (CPT) at Lansdowne Park suggest that the soil profile at this site includes a silt cap typically between 2.0 to 2.5 m thick, underlain by silty sand, and with the water table between 1.4 to 2.0 m below the ground surface. Wet sieve analyses (carried out in general accordance with ASTM D422-63(2007)e2) were performed on the ejecta specimens recovered from the locations shown in Figure 4.8. In general, the particle size distributions can be separated into two groupings. LDP-3, 4, 5, 8, 9 and 10 are relatively similar fine sands; whereas the samples LDP-1, 2, 4, 6 and 7 are medium sands. The particle size distributions of these two groups are summarised in Figure 4.9.

Historical maps from 1895 indicate that the north-east corner of the site lies in the river channel of that time, which has since been abandoned (Cook, 1895). In particular, the line of ejecta features starting from LDP-6 and moving south east towards LDP-2 in Figure 4.8 correlate closely with the southern edge of the river channel circa 1895. Historic photos show that this area was already filled by 1938 (Marlborough District Council 2017), but the position of the former river channel is indicated by a topographic depression and markings in the vegetation. Additional liquefaction ejecta features were discovered within paleo-channels in the former flood plain to the west of the park (Figure 4.10).

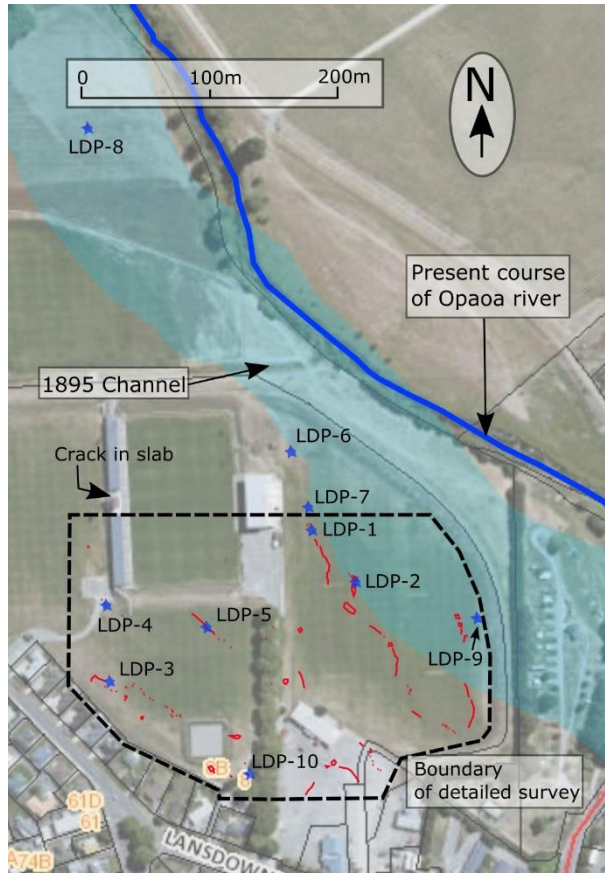


Figure 4.8: Location of ejecta at Lansdowne Park designated by red regions, with sample locations designated by blue stars. The present course and the abandon channel of the Opaoa River are designated by a blue line and blue shading, respectively (approx. centre of image: S41.4980, E173.9587).

The sand boils discovered at Lansdowne Park were typically of the order of 1-2 m in diameter, and in many cases formed linear features, as shown in Figure 4.8, with a typical example shown in Figure 4.11. In a few limited locations, larger ejecta features of around 25 m<sup>2</sup> (plan area) were observed (Figure 4.12). Liquefaction ejecta were not observed around the edges of the foundations of the main stadium buildings. Small features were observed on the earthen bank on the south edge of the stadium (i.e. at the locations of LDP-4 and LDP-5 shown in Figure 4.8). Additionally, a small amount of ejecta was located at the base of a floodlight tower, as shown in Figure 4.13.

The only readily observable damage to the permanent structures at Lansdowne Park was a crack in the concrete foundation slab running east-west at the location of the stadium entrance, mid-way along the western stand (Figure 4.14).

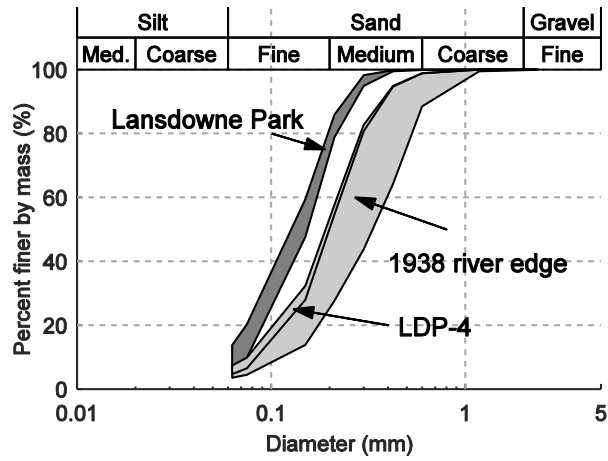


Figure 4.9: Particle size distributions of ejecta samples at Lansdowne Park.

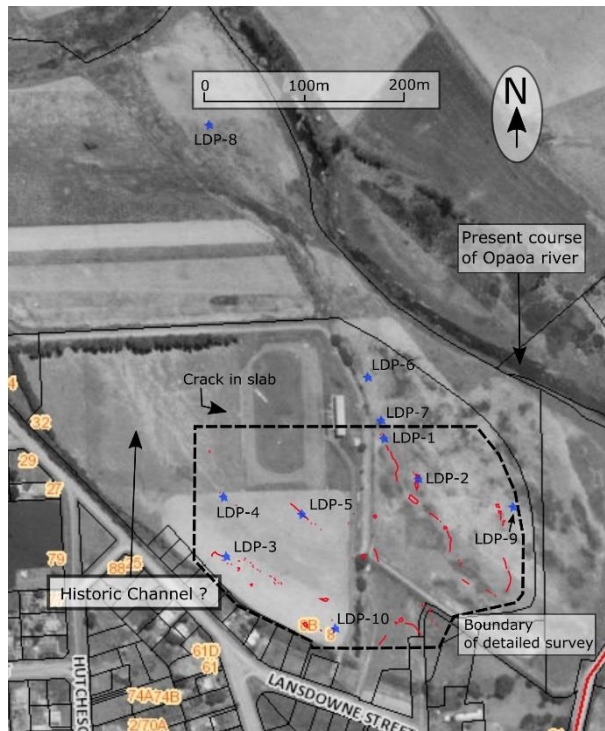


Figure 4.10: Locations of ejecta at Lansdowne Park overlaid on 1938 Photograph (approx. centre of image: S41.4980, E173.9587) (Marlborough District Council, 2017).



Figure 4.11: Linear liquefaction feature at Lansdowne Park (close to location of sample LDP-1, S41.4990, E173.9586, looking SE, 17 Nov 2016).



Figure 4.12: Largest liquefaction feature at Lansdowne Park (17 Nov 2016, S41.4996, E173.959, facing W).



Figure 4.13: Liquefaction ejecta at flood light tower (17 Nov 2016, S41.5003, E173.9572, facing N).



Figure 4.14: Crack in foundation slab on west stand (17 Nov 2016, S41.4993, E173.9569, facing E).



Figure 4.15: Cracking adjacent to the southern pier of the Opawa River Bridge (14 Nov 2016, S41.5006, E173.9616, facing N).

To the east of Lansdowne Park there was evidence of lateral spreading and grey sand ejecta running through the Top 10 Holiday Park and beneath the southern end of the Opaoa River Bridge (Location 2 in Figure 4.5). These features also seem to align with the position of the 1895 river channel described previously. Ground cracking was evident adjacent to the piers of the Opawa River Bridge as shown in Figure 4.15, with a few centimetres of settlement and horizontal displacement recorded.

#### 4.1.1.3 Park Terrace

Moderate volumes of liquefaction ejecta and lateral spreading were observed at an inner-meander bend of the Opaoa River north of Park Terrace, just downstream from the confluence of the Opaoa and Taylor Rivers (Location 4 in Figure 4.5). A summary of the damage at the site is presented in Figure 4.16, with both the riverbanks and the adjacent properties being affected. At this location, the ground between the southern bank of the Opaoa River and the northern edge of the industrial properties was relatively level (Figure 4.17). The ground then steeply slopes upward to form the stopbanks, and behind this the ground is again relatively flat heading back towards the road to the south (Figure 4.19). Damage to the opposing northern bank was inferred from drive-by surveys but was not confirmed by ground reconnaissance due to time constraints.

A hand auger adjacent to the river shown in Figure 4.16 indicated that the soil profile at this site is composed of a silt cap typically 2.2 m thick, underlain by fine-medium sand with trace silt, and the water table is approximately 1.5 m below the ground surface.

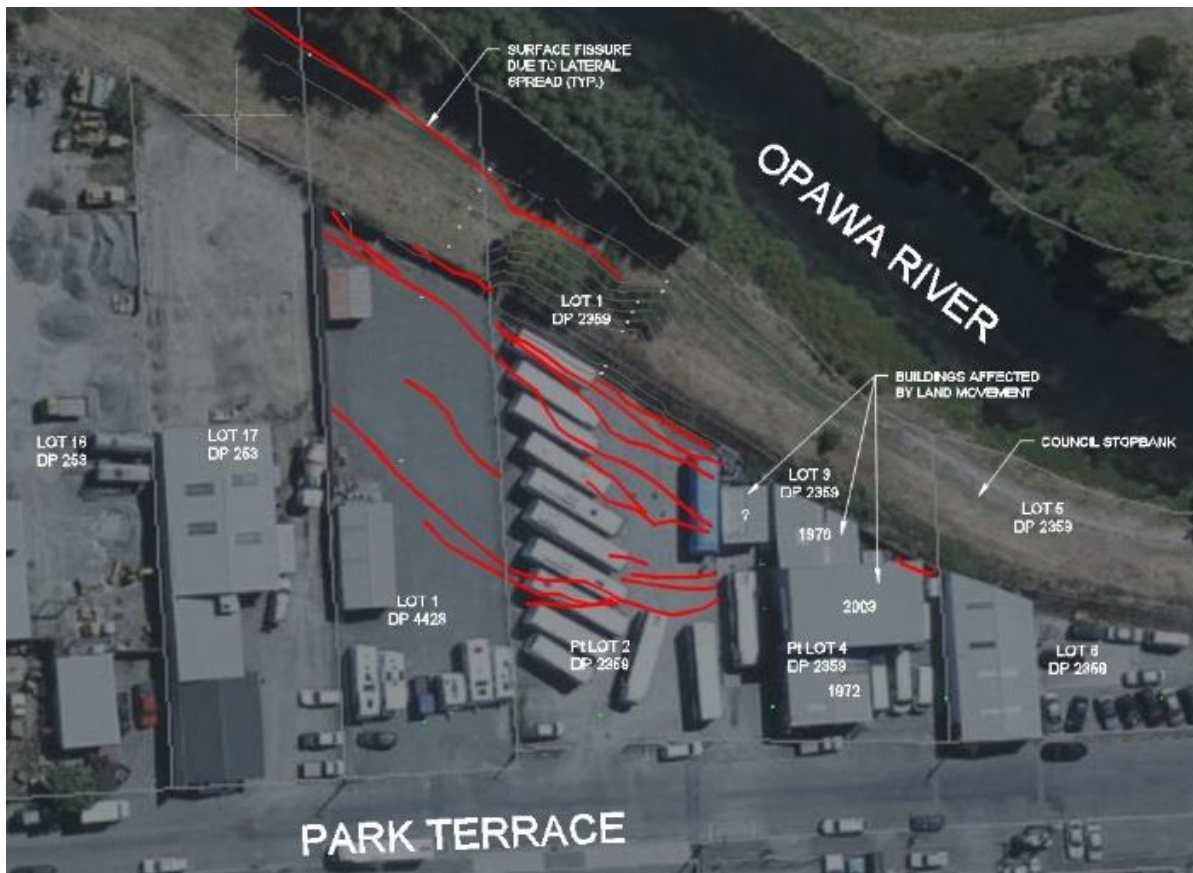


Figure 4.16: Summary of damage at the Park Terrace site. Dashed line indicates location of the historic stopbank (approx. centre of image: S41.5122, E173.9649).

Lateral spread cracks were evident along the river bank, and trees in the area were inclined towards the river suggesting movement towards the open face. The cracks were orientated sub-parallel to the river bank and covered the area extending from the river bank to the base of the stopbank. Cracks ranged in width from a few centimetres to as large as 30 cm (Figure 4.17) and were associated with approximately 1 to 5 cm of vertical settlement. Crack widths decreased with increasing distance from the apex of the inner meander bend and became discontinuous along the river bank further upstream. A block drop of 15-20 cm was also identified in the area. Fine-medium grey sand ejecta up to 10 cm thick was evident in this area and filled many of the lateral spreading cracks (Figure 4.18).

Lateral spreading/deep seated slumping and vertical displacement were observed within the properties on Park Terrace bordering the stopbank, with the location of the cracking summarised in Figure 4.16. Historic photos indicate that the lateral spreading/deep seated slumping in these properties was confined to the areas between the southern river bank and the location of the original stopbanks in this area. The properties affected were constructed on fill that raised the elevation of the zone between the historic stopbanks and the existing stopbanks to the south.



Figure 4.17: Crack parallel to Opaoa River surrounded by grey ejecta to the north of the Park Terrace properties (7 Dec 2016, S41.5121, E173.9651, facing E).



Figure 4.18: Ejecta at the base of the Park Terrace stopbanks (5 Dec 2016, S41.5121, E173.9651, facing E).



Figure 4.19: Ground damage to industrial properties along Park Terrace (5 Dec 2016, S41.5122, E173.9649, facing SE).

Cracks propagated across a number of properties, resulting in permanent ground deformation, differential settlement of structures, separation between foundation slabs and the surrounding ground, and damage to the stopbanks. Details of the cracking are shown in Figure 4.16, Figure 4.19 to Figure 4.21 and Table 4.1.



(a)



(b)

Figure 4.20: Examples of cracks along Park Terrace properties (5 Dec 2016): S41.5122 E173.9649, facing E; (b) S41.5121, E173.9647, facing W.

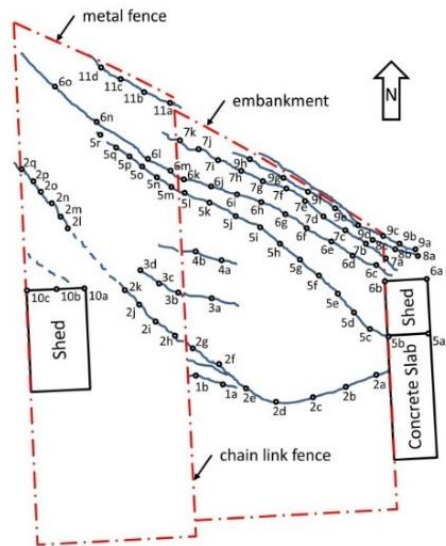
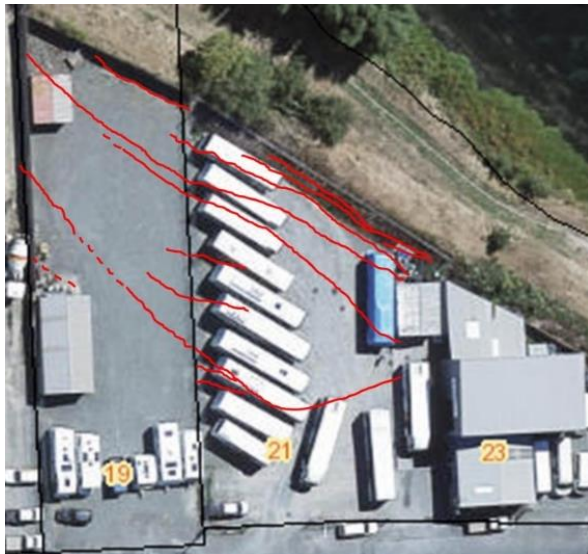


Table 4.1: Horizontal and Vertical (H:V) displacements measured at locations of Figure 4.21.

location	H:V(mm)	location	H:V(mm)	location	H:V(mm)	location	H:V(mm)	location	H:V(mm)												
1a	100:10	2a	10:0	3a	40:0	4a	50:0	5a	130:0	6a	100:20	7a	0:0	8a	0:0	9a	220:0	10a	80:50	11a	400:130
1b	50:50	2b	140:4	3b	60:70	4b	60:0	5b	180:0	6b	130:0	7b	160:0	8b	250:0	9b	120:0	10b	30:60	11b	350:160
-	-	2c	140:0	3c	40:60	-	-	5c	0:0	6c	110:40	7c	170:40	8c	0:0	9c	40:0	10c	0:30	11c	450:190
-	-	2d	190:50	3d	0:0	-	-	5d	40:0	6d	100:10	7d	140:40	-	-	9d	30:0	-	-	11d	190:215
-	-	2e	290:80	-	-	-	-	5e	80:20	6e	60:0	7e	160:80	-	-	9e	50:0	-	-	11e	
-	-	2f	120:100	-	-	-	-	5f	60:40	6f	60:0	7f	130:60	-	-	9f	20:0	-	-	-	-
-	-	2g	40:100	-	-	-	-	5g	50:0	6g	50:0	7g	150:20	-	-	9g	80:0	-	-	-	-
-	-	2h	50:0	-	-	-	-	5h	50:0	6h	50:40	7h	160:-50	-	-	9h	30:-30	-	-	-	-
-	-	2i	150:30	-	-	-	-	5i	30:30	6i	60:10	7i	180:-90	-	-	-	-	-	-	-	-
-	-	2j	400:60	-	-	-	-	5j	0:0	6j	60:0	7j	120:-110	-	-	-	-	-	-	-	-
-	-	2k	210:60	-	-	-	-	5k	150:60	6k	70:-20	7k	180:-90	-	-	-	-	-	-	-	-
-	-	2l	0:0	-	-	-	-	5l	100:90	6l	150:0	-	-	-	-	-	-	-	-	-	-
-	-	2m	60:0	-	-	-	-	5m	110:0	6m	50:0	-	-	-	-	-	-	-	-	-	-
-	-	2n	110:0	-	-	-	-	5n	170:0	6n	130:140	-	-	-	-	-	-	-	-	-	-
-	-	2o	170:0	-	-	-	-	5o	80:0	6o	200:300	-	-	-	-	-	-	-	-	-	-
-	-	2p	320:0	-	-	-	-	5p	120:0	-	-	-	-	-	-	-	-	-	-	-	-
-	-	2q	380:0	-	-	-	-	5q	180:10	-	-	-	-	-	-	-	-	-	-	-	-
-	-	-	-	-	-	-	-	5r	0:0	-	-	-	-	-	-	-	-	-	-	-	-

#### 4.1.1.4 Elizabeth Street

Moderate lateral spreading was observed at a site on an inner meander bend of the Opaao River at the end of Elizabeth Street, affecting a footbridge and a residential property (Location 5 in Figure 4.5). The meander at this location had the tightest radius of all locations along the rivers in the Blenheim urban area. At this location, the ground slopes up away from the river with an elevation difference of 3.5 m between the riverbanks and a house. A summary of the damage at the site is presented in Figure 4.22.

A hand auger (HA1) adjacent to the river shown in Figure 4.22 indicated that the soil profile had a light brown silt with some sand to a depth of 1.2 m, underlain by fine blueish grey sand to 1.4 m. Below this was blueish grey fine-medium sand, with particle size distribution characteristics shown in Figure 4.7. The water table was at a depth of 1.0 m at this location. Further up the slope from the river banks near the house (HA2) the water table was at a depth of 2.0 m, with the bluish grey fine-medium sand at 2.4 m depth. The ejecta were uniformly composed of grey fine-medium sand and the particle size distributions of these ejecta are shown in Figure 4.7 (EC-1).

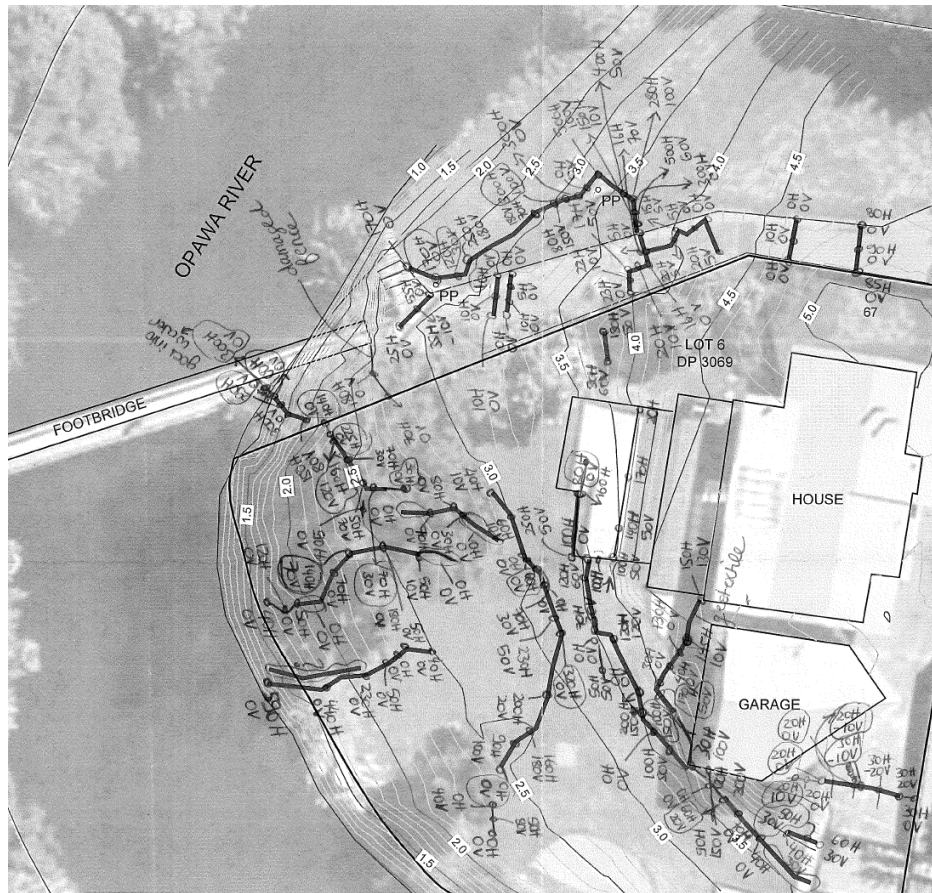


Figure 4.22: Summary of cracking and liquefaction manifestations at the Elizabeth St site (approx. centre of image: S41.5046, E173.9634).

The lateral spreading/slumping cracks in the area was oriented approximately parallel to the riverbanks on either side of the apex of the inner bank of the meander bend. Cracking orientated perpendicular to the river bank occurred at the apex of the meander bend. A summary of the lateral and horizontal displacement across the cracks is presented in Figure 4.22, with up to 50 cm of horizontal displacement and 10 cm of vertical displacement recorded. Cracks were up to 1 m in depth. Near the edge of the river the lateral spreading cracks extended to the water table and were filled with blueish grey fine-medium ejecta. A significant number of roots crossed through the cracks that were oriented perpendicular to the river and may have acted to reduce the severity of the cracking in this area (Figure 4.23).

Lateral spreading/deep seated slumping resulted in damage to the eastern end of the footbridge shown in Figure 4.24. The footbridge had two piers and steel I-beam girders with a wooden deck. The bridge deck warped as a result of the abutment having separated from the footpath by approximately 50 cm due to the lateral movement of the banks (Figure 4.24). A steel water main and an asbestos cement (AC) pipe crossed the river. The steel water main experienced movement but was not damaged, while the AC pipe had cracked and separated adjacent to the abutment.

To the south of the footbridge, cracks in the ground extended from the river up to the house on the property resulting differential movement and settlement of the house and cracks in the brick facade. The western side of the house and the garage moved relative to rest of the structure, resulting in warping of the frame and façade damage. This house was subsequently deemed unsafe for permanent occupancy; it was the only house in Blenheim red-tagged due to liquefaction related damage (Figure 4.25).



Figure 4.23: Crack at Elizabeth Street perpendicular to river filled with bluish-grey ejecta and intersected with roots (7 Dec 2016, S41.5088, E173.9635, facing E).



Figure 4.24: Damage to footbridge abutment at the end of Elizabeth Street (17 Nov 2016, S41.5087, E173.9636, facing W).



Figure 4.25: System of lateral spreading/slumping cracks at Elizabeth Street (7 Dec 2016, S41.5089, E173.9636, facing E).

Between the Lansdowne Park area and Park Terrace, Location 6 in Figure 4.5 was the only other site along the Opaoa River with evidence of liquefaction-related damage. This site was on the inner bank of a meander bend in the river and only experienced minor lateral spreading that had no impact on nearby structures (Figure 4.26).



Figure 4.26: Minor lateral spreading adjacent to the Opaoa River (6 Dec 2016, S41.5046, E173.9633, facing E).

### 4.1.2 Wairau Plains

Reconnaissance surveys and discussions with local engineers and Marlborough District Council provided a comprehensive summary of the liquefaction related impacts in the Wairau Plains near the coast. Figure 4.27 shows the locations of these impacts based on ground surveys and a robust set of aerial photos taken from a helicopter. The region bounded by the dashed lines indicates the area covered by the surveys, such that all locations within this area where no impacts are shown are unlikely to have any significant liquefaction manifestations.

In the greater Wairau Plains, outside the Blenheim urban area, the liquefaction mainly occurred in zones along the Wairau and Opaoa Rivers. The majority of the impacts of liquefaction were confined by the current stopbank network, with little evidence of liquefaction manifestation observed on the landwards side of the stopbanks. An overview of the damage to the stopbank network is provided in Figure 4.28, with some of these sites discussed in more detail in subsequent sections. Comparison of the observed damage with historical aerial photos of the area suggests that the stopbank damage can be related to the position of paleo-channels and associated swamps. The damaged sections were built on geologically younger deposits, with the adjacent undamaged sections being constructed on older deposits.

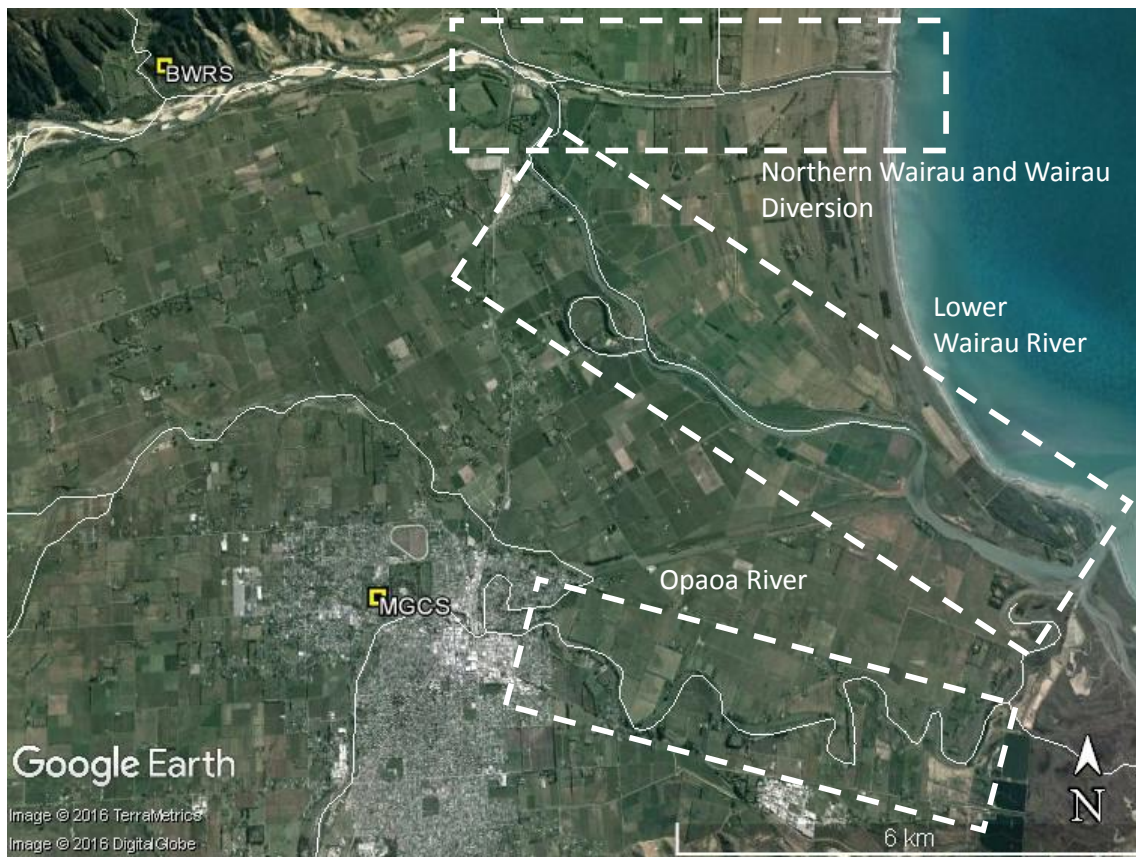


Figure 4.27: Overview of the Wairau Plain region and areas of focus outlined in subsequent sections (approx. centre of image: S41.4913, E173.9670).

Of the 180 km length of stopbanks, only 2.5 km were damaged to varying levels of severity across 18 sites. The damaged stopbanks tended to move towards the free-face of the river bank. Horizontal and vertical displacements varied significantly within the failure zone, ranging from a few centimetres to over 1 m. Displacements were accommodated through the development of systems of cracks, usually located on top of the stopbanks and running parallel to the free face of the river bank, with the ground between the cracks and the free face moving as a rigid block.

Accompanying phenomena, which were not observed in all cases, included the development of secondary systems of ground cracks or sand ejecta at the base of the stopbanks. These secondary features, when present, were parallel to the primary system of cracks.

Thirty pump stations for water control are situated in the Wairau Plains, and only three of which suffered relatively minor damage due to liquefaction.



Figure 4.28: Overview of the stopbank network on the Wairau Plains and locations of damage identified by red markers. Orange are the main stopbanks and yellow are the secondary stopbanks (approx. centre of image: S41.4913, E173.9670).

#### 4.1.2.1 Northern Wairau River and the Wairau Diversion

Figure 4.29 provides a summary of the liquefaction related damage in the Northern Wairau River and Wairau Diversion area. The damage mapping was developed from ground reconnaissance and helicopter photos.

Lateral spreading affected the Wairau River Bridge on State Highway 1 (Location 4 in Figure 4.29), resulting in ground cracking at the abutments and piers and horizontal cracking across the base of the abutment and pier walls. There was also approach slumping at the bridge at location 5 in Figure 4.29. Stopbank damage was identified at Spring Creek (Location 6 in Figure 4.29) and to the west of Hillocks Rd (Location 7 in Figure 4.29). The most severe stopbank damage in this area is summarised in the following sections.

#### 4.1.2.2 Wairau Diversion Stopbanks

The Wairau Diversion was constructed in the 1960's to mitigate the effects of flooding on the Wairau River by diverting a portion of the flow of the river away from the Blenheim Township to a direct path towards the coast. Along the Wairau Diversion, lateral spreading-induced or slumping-induced cracking was observed on both the north and the south banks aligned with a paleo-stream channel and swamp, recognizable due to a depression in the landscape and a change in vegetation on both sides of the diversion channel (Location 1 in Figure 4.29 and Figure 4.30). The swamp was present at the time the diversion was built, as indicated by historical conceptual drawings dating back to the first plans for the diversion (Figure 4.31). No other liquefaction or lateral spreading/slumping damage was observed adjacent to the northern or southern banks of the Wairau Diversion between this location and the Equestrian Park outlined in the following section.

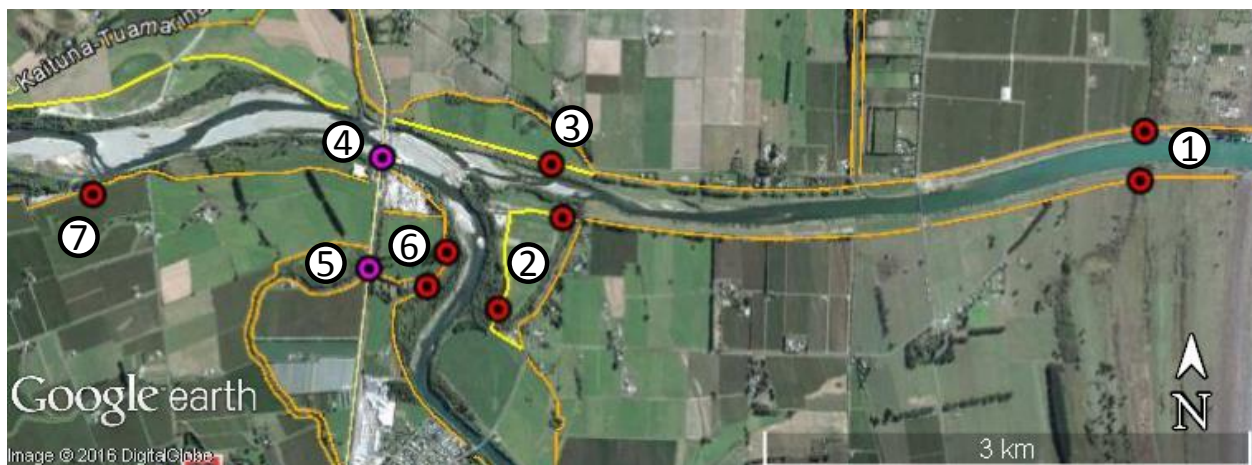


Figure 4.29: Map of liquefaction related damage in the northern Wairau River and Wairau Diversion area. Orange are the main stopbanks, and yellow are the secondary stopbanks. (approx. centre of image: S41.4484, E173.9831)

Lateral spreading and slumping of the northern stopbank was characterised by cracking along the top of the stopbank (Figure 4.32). The cracks ranged in width from approximately 30 to 50 cm and were associated with 10 to 50 cm of vertical settlement (Figure 4.33). The cracks all ran sub-parallel to the closest bank of the river. Localized cracking, approximately 2 to 10 cm wide, was observed at the base of stopbank proximal to the river (Figure 4.34a). No liquefaction ejecta were observed at the site, and no liquefaction induced damage was observed proximal to a culvert exiting the stopbank at the easternmost extent of the affected area (Figure 4.34b).

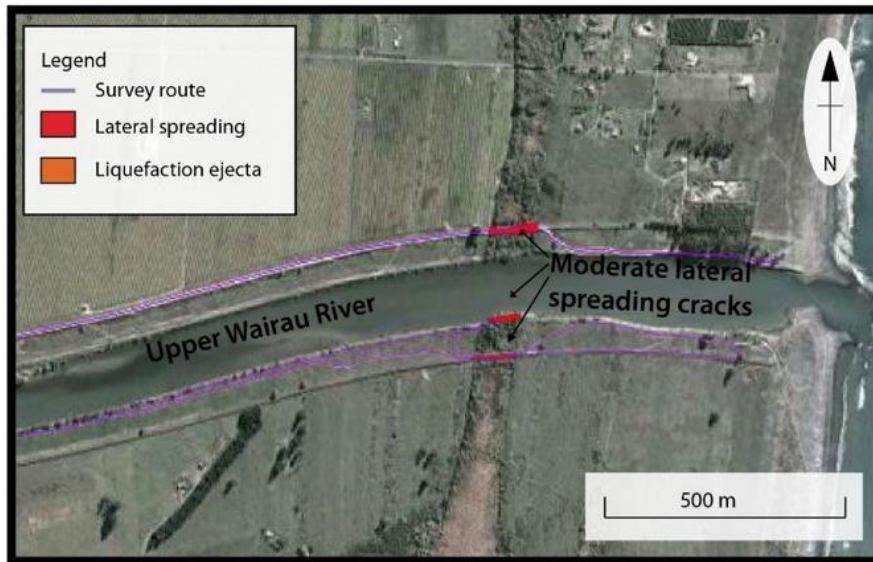


Figure 4.30: Summary of damage observations along the Wairau Diversion (approx. centre of image: S41.4401, E174.0206).



Figure 4.31: Historical drawing of Wairau Diversion. The dotted regions indicate locations of swamps, with the location of failed stopbank highlighted in red (approx. centre of image: S41.4401, E174.0206, Marlborough Catchment Board, 1959)

This site was scanned using a terrestrial LiDAR scanner (Optech, Inc. ILRIS-3D laser scanner) on 6 December 2016. Four scans were performed from the approximate locations shown in Figure 4.35. The data from the scans are still being processed, but will result in a three-dimensional point cloud that will allow cm-scale determination of horizontal and vertical displacements of the stopbank due to lateral spreading or slumping.



Figure 4.32: Lateral spreading induced cracking along top of northern stopbank (17 Nov 2016, S41.4387, E174.0214, facing E).



Figure 4.33: Maximum vertical settlements of 50 cm were observed along the cracks in the northern stopbank (17 Nov 2016, S41.4386, E174.0216, facing N)

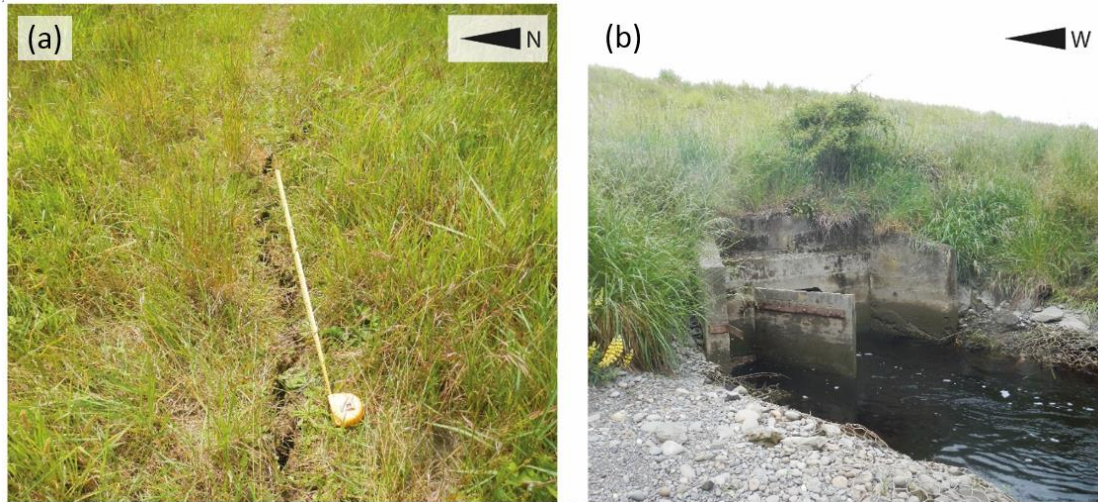


Figure 4.34: a) Cracking observed along the base of the northern stopbank proximal to the river (17 Nov 2016, S41.4390 ,E174.0220, facing E); b) No liquefaction induced damage was observed within the culvert exiting the northern stopbank (17 Nov 2016, S41.4387, E174.0223, facing NE).



Figure 4.35: Approximate locations of four LiDAR scans performed on 6 Dec 2016 (approx. centre of image: S41.4387, E174.0218).

Lateral spreading along southern bank also resulted in cracking along the top of the stopbank (Figure 4.36), although not as severe as the damage on the northern stopbank. The affected area extended for approximately 60 m along the stopbank and consisted of a series of sub-parallel cracks that varied in width from approximately 10 to 40 cm. The cracks exhibited approximately

10 to 40 cm of vertical settlement. No cracking was observed along the base of the stopbank, and no liquefaction ejecta were observed at the site.

Lateral spreading or ground slumping also resulted in cracking of the southern bank of the river (Figure 4.37a). The affected area extends approximately 30 m along the river bank and approximately 3 m inland, with no further cracking observed within the vegetation distal to the river. The cracks range in width from approximately 50 to 60 cm and are associated with 1 to 10 cm of vertical settlement (Figure 4.37b). No liquefaction ejecta were observed at the site.



Figure 4.36: Cracking along the top of the southern stopbank of the Wairau Diversion (Tape set at 1 m) (17 Nov 2016, S41.4414, E174.0219, facing W)



Figure 4.37: Cracking of the southern bank of the Wairau Diversion: (a) 17 Nov 2016, S41.4406, E174.0215; (b) 17 Nov 2016, S41.4406, E174.0215.

#### 4.1.2.3 Marlborough Equestrian Park

The Marlborough Equestrian Park was opened in 2014 and is the home of equestrian sports in Marlborough. It is located NE of Blenheim and is bounded in the west by the Wairau River, in the north by the Wairau Diversion, and in the east and south by a stream that is a remnant of a historic channel of the Wairau River (Location 2 in Figure 4.29). An overview of the site is provided in Figure 4.38. Stopbanks surround the park, with the stopbanks to the east of the park forming part of the main flood defence network of the region and the rest of the stopbanks being part of the secondary protection network. The park itself is relatively flat, with a gradual reduction in elevation of the ground surface moving from north to south.

Hand augers (HA1 and HA2) performed adjacent to the remnant river channel (where the path intersects with Group B cracks in Figure 4.38) shown in indicated that the soil profile had a light brown silt stratum with some sand to a depth of 2.8 m. Below this was blueish grey fine-medium sand, having the particle size distribution shown in Figure 4.66; particle size distribution curves for samples from other locations along the Wairau River are also shown in Figure 4.66. The water table was at a depth of 1.5 – 2.0 m at the two hand auger locations.

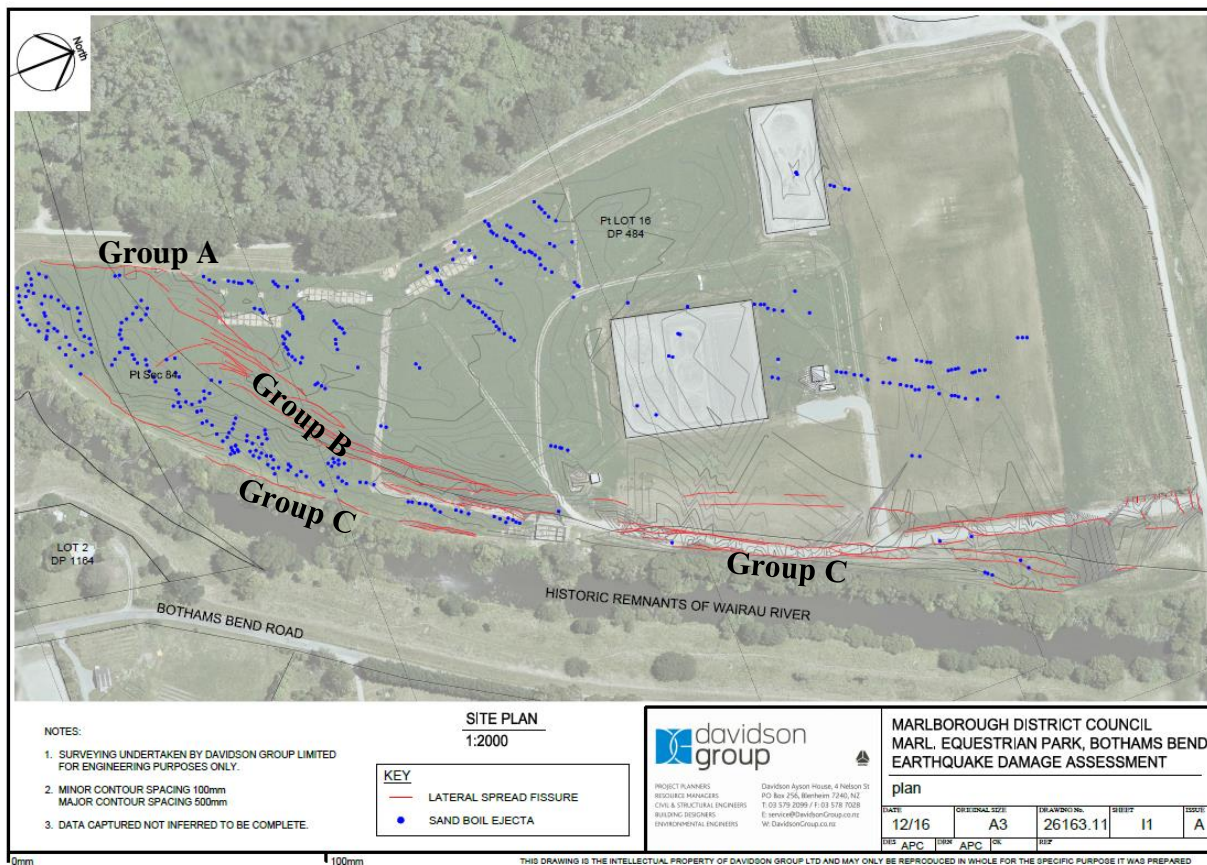


Figure 4.38: Overview of liquefaction induced damage at the Marlborough Equestrian Park (approx. centre of image: S41.4455, E173.9761) (courtesy of Davidson Group)

Figure 4.38 provides a detailed summary of the lateral spreading and liquefaction features across the park, and Figure 4.39 provides an aerial overview of the damage, with extensive lateral spreading, differential settlement, deformation of pavement, and extensive sand boils observed at the site. The red lines represent lateral spreading cracks and the blue dots represent sand boils. This detailed map was developed by Davidson Group and the GEER team after the earthquake. The southern part of the park was more affected by the earthquake than the northern part of the park. It is possible, however, that the mapping of some cracks and sand boils in the northern part of the park was obscured by vegetation

Extensive mapping and surveying of lateral spreading and ejecta were carried out by the reconnaissance team and local engineers. Cracking and ejecta is aligned with the location of the historic Wairau River channel prior to the construction of the Wairau Diversion in the 1960's.

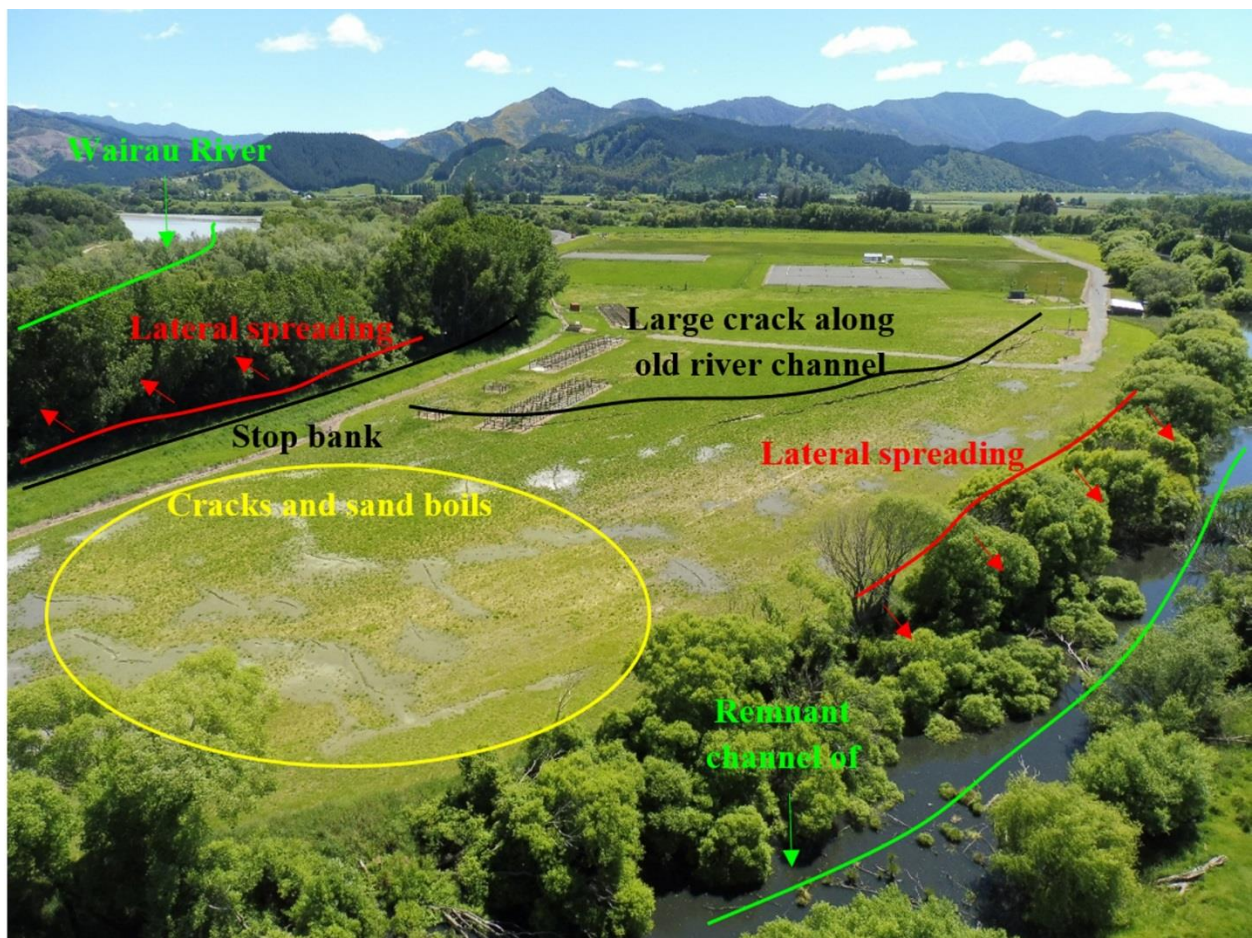


Figure 4.39: Aerial view of Marlborough Equestrian Park (14 Nov 2016, S41.4474, E173.9768, facing NE, Marlborough District Council 2016).

In Figure 4.38, lateral spreading cracks are organised into three groups: Group A cracks ran parallel to the secondary stopbanks on the western edge of the park, Group B cracks were oriented in the SW-NE direction and ran along the edge of the infilled historic river channel; and Group C cracks which run parallel to the stream that is remnant of the historical river channel. The elevation of the ground surface gradually reduced moving south, which correlates with the increase in severity of the lateral spreading.

Group A cracks had a NNE-SSW orientation and were characterized by small to medium horizontal openings (~10-30 cm) with little to no vertical displacement (< ~10 cm). The cracking followed along the base of both sides of the secondary stopbank (Figure 4.40) in areas that used to be part of the Wairau River bed and have since been infilled. The cracks cut through the stopbank where the infilled historic river channel that ran along the east and south of the park merged Wairau River channel that runs north-south. Grey ejecta were present both in the cracks and adjacent to the cracks.

Group B cracks, the most significant crack system in the park, were oriented in the NE-SW direction and were characterized by small to large openings (~10-70 cm) and up to ~70 cm vertical displacement (Figure 4.41a). In this area there was settlement of the ground surface within the infilled historic channel, with the largest cracks aligning with the northern bank of the historic channel (Figure 4.38). Cracking propagated out from this main crack in both directions, with the cracking related to the slumping more than to significant global lateral movement (Figure 4.41b). The cracks in this area were filled with grey ejecta. Further evidence that this cracking followed the infilled historic channel is the coincidence of this cracking with the strip of lush vegetation shown in Figure 4.42.



Figure 4.40: Group A cracking along the base of the secondary stopbanks (4 Dec 2016, S41.4487, E173.9738, facing NE).

The portion of the Group B lateral spread cracks that crossed the dirt access road to the Equestrian Park was scanned using a terrestrial LiDAR scanner (Optech, Inc. ILRIS-3D laser scanner) on 5 Dec 2016. Six scans were performed from the approximate locations shown in Figure 4.43. The data from the scans are still being processed. They will produce a three-dimensional point cloud that will allow cm-scale determination of horizontal and vertical displacements of the lateral spreading features.



(a)



(b)

Figure 4.41: Most severe lateral spreading at the Equestrian Park with 70 cm of vertical offset, with ejecta in the crack: (a) facing NE (b) facing NW (5 Dec 2016, S41.4474, E173.9760).

Group C cracks were oriented in the NE-SW direction and were characterized by small to medium horizontal openings (~10-20 cm) and little to no vertical displacement (< ~10 cm). These cracks aligned with the remnant stream channel and movement was to the east towards this channel. Thick foliage along the riverbanks likely obscured other cracking in this area. However, the submerged trees at the bottom right corner of Figure 4.39 provide evidence of more lateral spreading of these banks.

At the north of the park the access road running along the secondary stopbank was fissured and cracked, and this cracking extended through to the Wairau Diversion channel to the north. Cracking was perpendicular to the road (i.e., cracking ran in the north-south direction; Figure 4.44) adjacent to and parallel with the historic river channel that existed prior to the construction of the Wairau Diversion in the 1960's. However, the cracking ran parallel to the road (i.e., in the east-west direction; Figure 4.45) where it crossed the historic channel as a result of the embankment slumping and spreading horizontally. At this location the crack were up to 10 cm wide.

Lateral spreading was accompanied with widespread sediment ejecta. The volume of ejecta was the most severe in the southern part of the park where the ground elevation was the lowest. The locations of the centres of the mapped sand boils are shown in Figure 4.38 and the volume of ejecta in this region can be seen in the aerial photograph in Figure 4.39, with ejecta up to 20 cm thick in places. In addition to sand boils, ejecta filled up many cracks (Figure 4.41 b). Examples of ejecta deposits are provided in Figure 4.46. Outside of the Equestrian Park, ejecta were also present in the lower lying areas to the north of the Equestrian Park between the stopbank and the Wairau Diversion.



Figure 4.42: Group B cracks following the historic river channel: (a) facing SW, and (b) facing E (4 Dec 2016, S41.4474, E173.9759). Note the lush vegetation strip identifies the location of the historic river channel.



Figure 4.43: Approximate locations of six LiDAR scans performed on 5 Dec 2016 (The black line is the approximate location of the largest lateral spread crack; approx. centre of image: S41.4477, E173.9760).



Figure 4.44: Crack at the entrance to the Equestrian park at edge of historic river channel (15 Nov 2016, S41.4436, E173.9790, facing W, Marlborough District Council 2016).



Figure 4.45: Cracks in the access road that crosses a historic river channel at the Equestrian Park (15 Nov 2016, S41.4436, E173.9790, facing E, Marlborough District Council 2016).



(a)

(b)

Figure 4.46: Examples of ejecta at the Equestrian Park (4 Dec 2016): (a) S41.4471, E173.9748, facing SW; (b) S41.4468, E173.9769, facing N.

#### 4.1.2.4 Blind Creek Stopbanks

At Blind Creek a primary and secondary set of stopbanks are present (Location 3 in Figure 4.29); the secondary set runs parallel to the current channel of the Wairau River while the primary stopbank is set back from the river outside of a cut-off meander bend of the river (Figure 4.47). A 200-m-long section of the secondary stopbank at Blind Creek was heavily damaged (Figure 4.47). The location of this stopbank falls within the historical bed of the Wairau River, with Blind Creek comprising a cut-off meander bend of the Wairau River associated with river avulsion and the construction of the Wairau Diversion in the 1960's.

An aerial view of the stopbank damage is presented in Figure 4.48. Cracks up to 1 m wide and 1 m deep developed along the stopbank (Figure 4.49), suggesting the development of slumping and horizontal displacements away from the major axis of the stopbanks in the north and south directions (Figure 4.47). Sand boils were observed on the foundation soils surrounding the stopbank closer to the river's edge and on the northern side of the stopbank within the paleo-channel (Figure 4.50). Slumping of the stopbank was also observed where Blind Creek flows underneath the stopbank through a culvert.

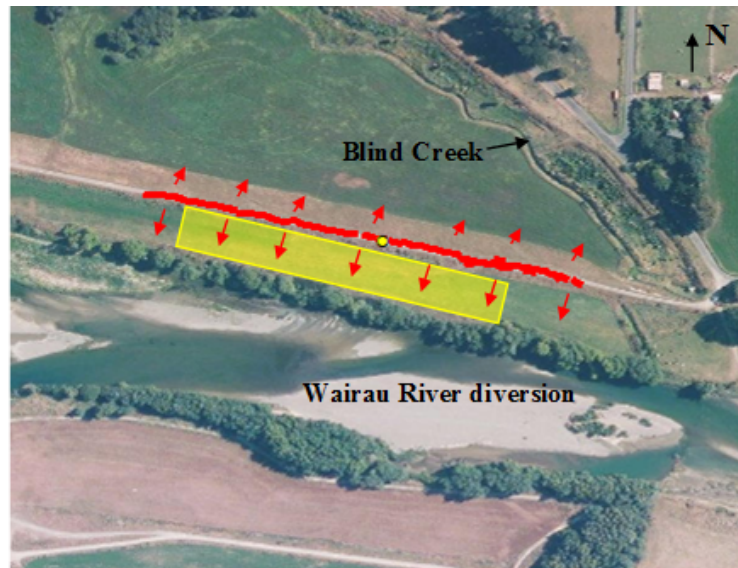


Figure 4.47: Overview of damage at Blind Creek Stopbank (approx. centre of image: S41.4405, E173.9762).



Figure 4.48: Aerial view of the Blind Creek stopbank damage (18 Nov 2016, approx. centre of image: S41.4405, E173.9762, Marlborough District Council 2016).



Figure 4.49: Damage to the secondary stopbank at Blind Creek (5 Dec 2016, S41.4407, E173.9791, facing W).



Figure 4.50: Cracks and ejecta on the foundation soil between the secondary stopbank and the river (5 Dec 2016, S41.440967, E173.980122, facing NE).

### ***4.1.3 Lower Wairau River***

Figure 4.51 provides an overview of the liquefaction related damage along the Lower Wairau River between the southern edge of the Equestrian Park and the coast and locations that are discussed in more detail. Particle size distributions of ejecta samples from along the Wairau River are presented in Figure 4.52. The damage mapping was developed from ground reconnaissance and aerial photographs taken from a helicopter.

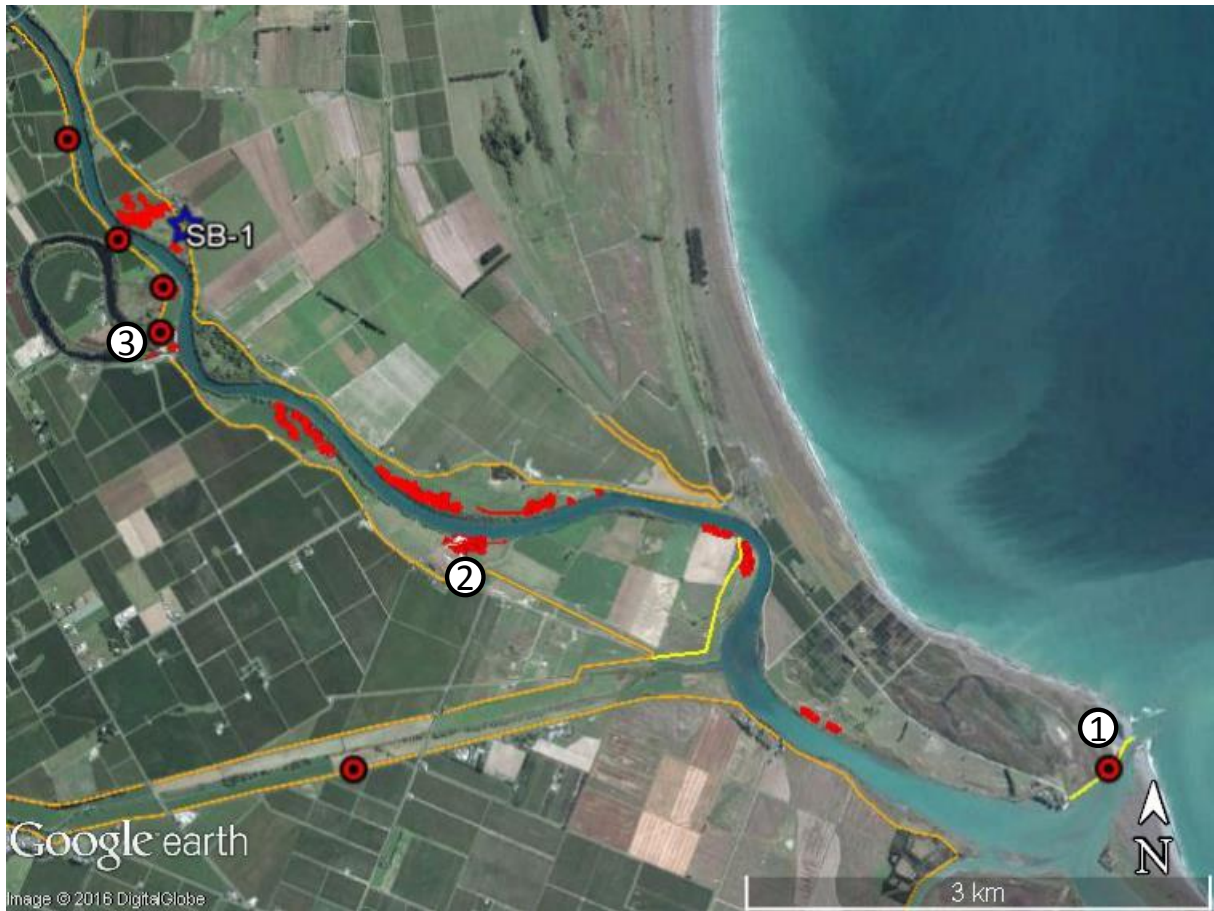


Figure 4.51: Aerial overview of the reconnaissance along the Lower Wairau River. Locations with detailed investigations are identified numerically, and locations where samples have been collected from are shown by blue stars. (Approx. centre of image: S41.4871, E174.0127).

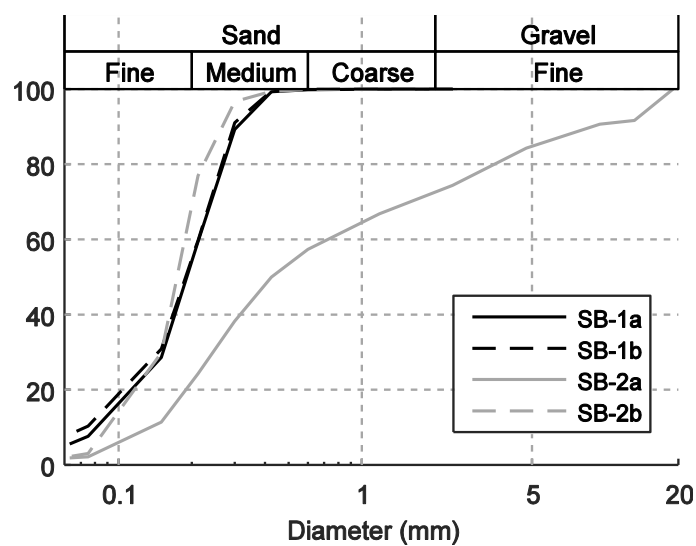


Figure 4.52: Particle size distributions of ejecta samples from the stopbanks along the Wairau River. Locations of these samples summarised in Figure 4.51.

#### 4.1.3.1 Banks of Lower Wairau River

Along the eastern bank of the lower Wairau River are a number of farms, vineyards, and a marae (Maori meeting grounds), with the main stopbank running the length of the river to the Wairau Bar. Severe lateral spreading and large volumes of liquefaction ejecta were observed proximal to the inner banks of the meander bends, and paleo-channels associated with cut-off meander bends. The liquefaction induced damage occurred between the stopbanks and the river bank, with no liquefaction or lateral spreading induced damage observed to the stopbanks or along the road outside of the stopbanks. It is possible that minor lateral spreading and associated liquefaction ejecta occurred along the river banks in this area, but liquefaction features may have been obscured during helicopter reconnaissance or not visited during ground reconnaissance mapping.

A summary of the damage along the lower Wairau River is presented in Figure 4.53. The liquefaction manifestations along the river both followed the old meanders of the river and were parallel to the existing river banks. Aerial views of this damage are presented in Figure 4.54 and Figure 4.55.



Figure 4.53: Summary of liquefaction induced damage along the banks of the Lower Wairau River, with red areas indicating cracking and ejecta locations. Stopbank damage is shown by the red symbols in this figure. (Approx. centre of image: S41.4799, E174.0006).



Figure 4.54: Lateral spreading and liquefaction ejecta on the eastern banks of the Lower Wairau River (18 Nov 2016, S41.4687, E173.9807, taken facing SE).



Figure 4.55: Lateral spreading and liquefaction ejecta on the eastern banks of the Lower Wairau River (18 Nov 2016, S41.4854, E174.0160, taken facing W).

Minor lateral spreading induced cracking was observed proximal to the river bank at 132 Wairau Bar Road (Figure 4.56a and b, location 1 in Figure 4.53). Although at the time of the reconnaissance the property had already been cleared by the owner, manifestations of liquefaction and lateral spreading-induced cracking were still recognizable. Cracking occurred in the area extending approximately 10 m inland from the river bank, and transitioned into a zone of localized elliptical liquefaction ejecta extending to the base of the stopbank. The lateral spreading cracks ranged in width from 10 to 50 cm and extended along the length of the river bank (Figure 4.56a). The cracks did not exhibit any ejecta but were associated with undulations

in the ground that were not present prior to the earthquake. The localized elliptical liquefaction ejecta features ranged from 10 to 20 m in length and 1 to 2 m in width. The features were uniformly composed of grey fine sand and were associated with 10 to 30 cm wide cracks that were orientated sub-parallel to the river bank.

A localized elliptical liquefaction ejecta feature, measuring approximately 8 m in length and 2 m in diameter, was observed in a ditch along the southern margin of the stopbank at 188 Wairau Bar Road (Figure 4.57a, location 2 in Figure 4.53). The feature was composed of grey fine sand which was still wet during the reconnaissance visit on 17 Nov 2016, and was associated with standing water in the ditch. Elliptical liquefaction ejecta features of similar dimensions were observed scattered throughout the adjacent farmland and were orientated sub-parallel with the river in this location (Figure 4.57b). The river bank was not surveyed at this location, but a neighbouring land owner indicated that lateral spreading induced cracking occurred within 10 m of the river bank, while localized ejecta were present at distances >10 m.

Localized cracking was also observed along the southern margin of the stopbank in the farmland opposite 515 Wairau Bar Road (Location 3 in Figure 4.53). The cracks were confined to the stopbank and range from 10 to 20 m in length and approximately 20 to 50 cm in width (Figure 4.58a). No liquefaction ejecta were observed associated with these cracks.

A series of localized elliptical liquefaction ejecta features were observed within the farmland extending from the base of the stopbank to the river bank (Figure 4.58b). The features range in length from 5 to 7 m and 1 to 2 m in diameter, and are uniformly composed of grey, fine sand. The river bank was not surveyed at this location; however, it is assumed that localized lateral spreading occurred within 10 m of the river bank.



Figure 4.56: a) Lateral spreading induced cracking was observed within 10 m of river bank at 132 Wairau Bar Road. b) Localized liquefaction ejecta associated with cracks were observed at distances >10 m from the stopbank (17 Nov 2016): (a) S41.4671, E173.9802, facing N; (b) S41.4675, E173.9808, facing N.



(a)



(b)

Figure 4.57: a) Liquefaction feature in ditch next to the stopbank at 188 Wairau Bar Road. b) Evidence of similar liquefaction features in adjacent farmland, between the stopbank and the river bank (both S41.468902, E173.986465, facing W).



(a)



(b)

Figure 4.58: a) Cracks within the southern side of the stop bank opposite 515 Wairau Bar Road. Features ranged in width from 20 to 50 cm (tape set at 1 m for scale). b) Liquefaction ejecta features within the farmland between the stop bank and river mouth (tape set at 1 m for scale). (17 Nov 2017): (a) S41.4843, E174.0147, facing N; (b) S41.4847, E174.01523, facing N.

#### 4.1.3.2 Wairau Bar

Lateral spreading was observed along Wairau Bar stopbank on the northern bank of the mouth of the Wairau River (Location 1 in Figure 4.51). An overview of the site is presented in Figure 4.59, where cracking was observed along an approximately 100 m long section of the stopbank. Historical aerial photos of the river mouth showed that the damaged section of the stopbank was built on an old river channel that ran parallel to the coast prior to the stopbank construction (Figure 4.60).

An aerial view of the damage is presented in Figure 4.61. The eastern and western termini of the affected area exhibited cracks that varied in width from approximately 2 to 5 cm and were associated with vertical displacements of 1 to 5 cm. The central affected area exhibited a series of sub-parallel cracks that varied in width from 30 to 50 cm and were associated with vertical settlements of 20 to 120 cm (Figure 4.62 and Figure 4.63). No liquefaction ejecta were observed in the cracks along the stopbank nor in the mudflats exposed within the river channel.



Figure 4.59: Top view of stopbank along Wairau River (centre of image S41.502404, E174.058915).

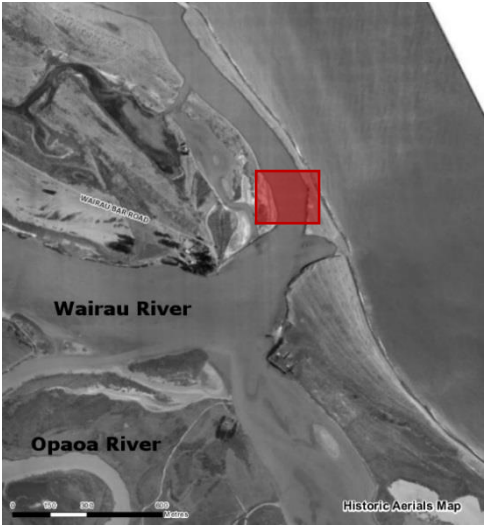


Figure 4.60: Aerial photo of the Wairau river mouth in 1948. In red: location of failed stopbank (centre of image S41.5027, 174.05777, Marlborough District Council 2017).



Figure 4.61: Aerial view of left stopbank at Wairau River mouth (18 Nov 2016, S41.5003, E174.0600, facing S, Marlborough District Council 2016).



Figure 4.62: Severe cracking of levee (17 Nov 2016, S41.50122, E174.060071, facing E).



Figure 4.63: Measurement of vertical relative displacement along crack, tape set at 150 cm (17 Nov 2016, S41.5012, E174.0603, facing N).



(a)



(b)

Figure 4.64: a) Cracks, running sub-parallel to the stopbank, with associated liquefaction ejecta along the northern (inland) margin of the stopbank. b) Fissure with associated liquefaction ejecta in a side road; the feature is orientated parallel to an adjacent small stream and perpendicular to the stopbank (17 Nov 2016): (a) S41.5005, E174.0607, facing E; (b) S41.5016, E174.0589, facing N..

A series of lateral spreading cracks were also observed along the inland (northern) margin of the stopbank and extended 15 to 20 m inland (Figure 4.64a). The cracks varied in width from 20 to 40 cm and were surrounded by liquefaction ejecta composed of grey fine sand. The features were observed on the road running along the base of the inland margin of the stopbank and were all orientated parallel with the stopbank.

A lateral spreading crack surrounded by liquefaction ejecta composed of grey fine sand was observed in a side road that runs perpendicular to the stopbank (Figure 4.64b). The feature was located adjacent and sub-parallel to a small stream that feeds into the Lower Wairau, and perpendicular to the cracking observed within the stopbank.

#### 4.1.3.3 Blenheim Rowing Club

The Blenheim Rowing Club (BRC) is located on the western bank of the Wairau River, and severe liquefaction manifestations and lateral spreading occurred in the area (Location 2 in Figure 4.51). This was the only location in the region where significant liquefaction related damage was present on the outer bend of a river. However, historic maps (Cook, 1895) and property boundaries show that there was an S-bend in the river in this area that was straightened (Figure 4.65). Much of the damage that occurred was confined to the boundaries of the paleo-channel. Figure 4.65 provides a summary of the damage in and around the rowing club, with large areas affected by lateral spreading and significant volumes of ejecta. A sample of ejecta was taken north of the main clubhouse building, and the particle size distribution is presented in Figure 4.66.

Aerial views of damage in the area presented in Figure 4.67 and Figure 4.68 provide a clear indication of the severity of damage in this area. Severe liquefaction ejecta were observed at the physical site of the rowing club and surrounding fields to the east and west of the rowing club. Sand boils were typically several metres in diameter and many linear arrays of sand boils were located across the site. Approaching the river, these lines of sand boils tended to become orientated parallel to the river, and in many cases, were associated with lateral spreading cracks.

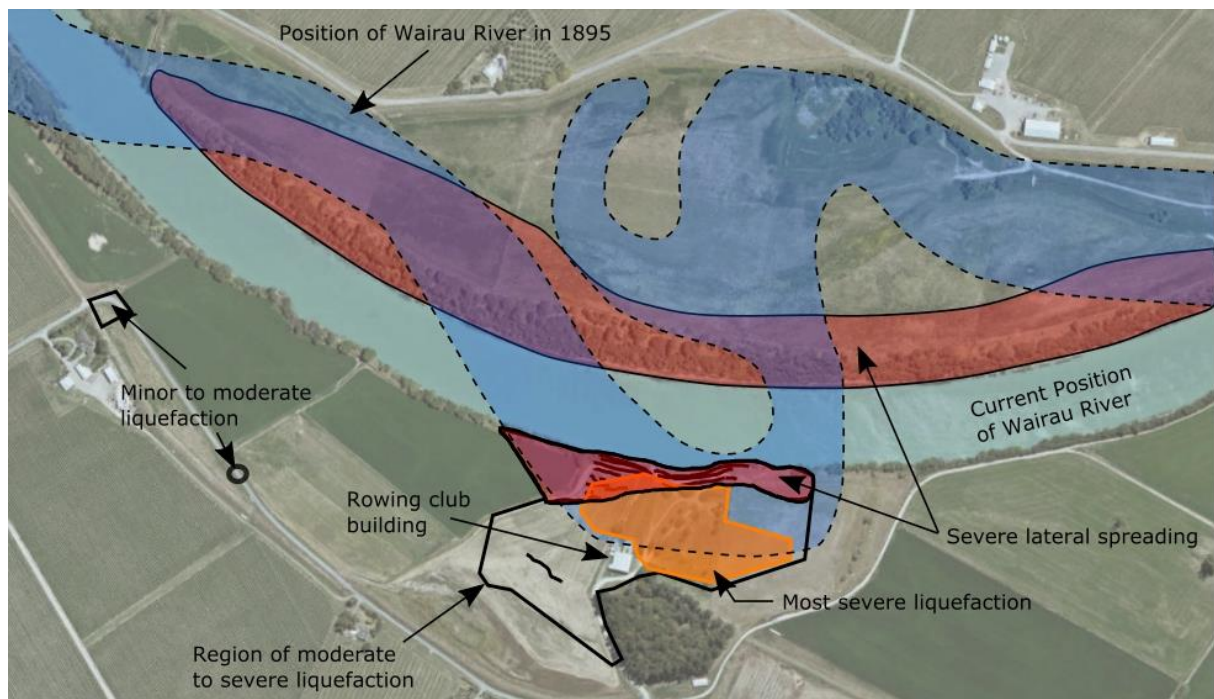


Figure 4.65: Summary of observations at Blenheim Rowing Club (approx. centre of image: S41.4860, E174.0105, Basemap: Marlborough District Council, 2017)

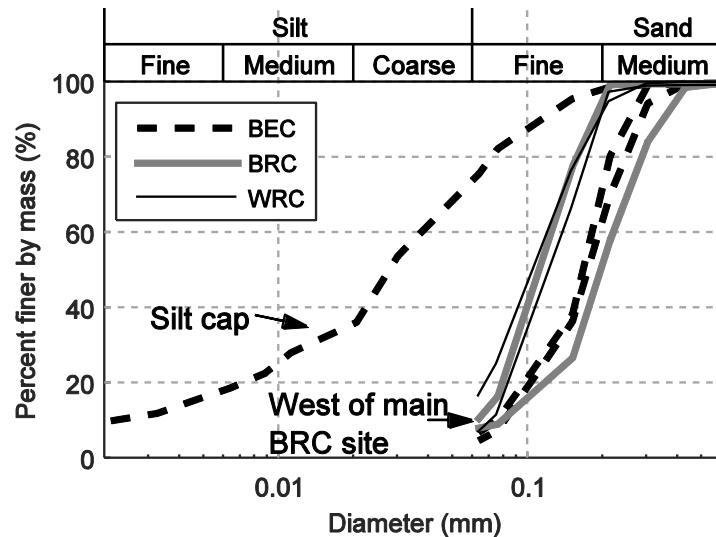


Figure 4.66: Particle size distributions of ejecta samples from along the Wairau River. (BEC=Equestrian Club (S41.4476, E173.9761), BRC=Blenheim Rowing Club (S41.4882, E174.0088), and WRC=Wairau Rowing Club (S41.5003, E174.0600)).



Figure 4.67: Aerial view of liquefaction manifestation at the Blenheim Rowing Club looking south (18 Nov 2016, approx. centre of image: S41.4890, E174.0094, Marlborough Regional Council, 2016).

Numerous lateral spreading cracks were observed at this site and varied in width from approximately 10 cm (at distances of approximately 60 m from the river) to over 1 m at locations close to the river channel (Figure 4.69 and Figure 4.70). Transects of the cumulative crack widths at this site summarized in Figure 4.71 and Table 4.2 show that lateral spreading displacements of the order 2-5 m accumulated over a horizontal distance of approximately 60 m from the river.



Figure 4.68: Aerial view of liquefaction manifestation at the Blenheim Rowing Club looking east (18 Nov 2016, approx. centre of image: S41.4883, E174.0096, Marlborough Regional Council, 2016).



Figure 4.69: Lateral spreading at the east end of the rowing club site. Note: measuring tape set to 1m. (17 Nov 2016, S41.4882, E174.0105, facing E).



Figure 4.70: Lateral spreading at the west end of the rowing club site. (17 Nov 2016, S41.4881, E174.0101, facing E).

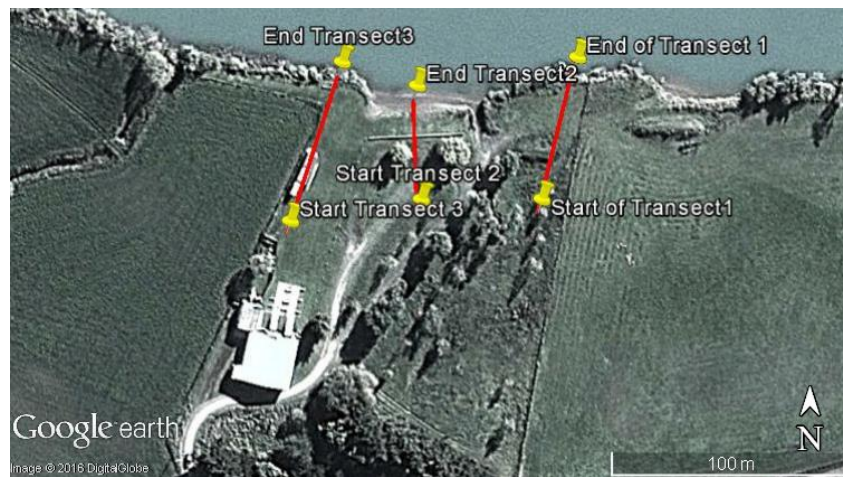


Figure 4.71: Transects where cumulative crack widths were measured to estimate lateral spreading displacements. (Approx. centre of image: S41.4886, E174.0102, Imagery from GoogleEarth).

Table 4.2: Summary of transects at Blenheim Rowing Club summarised in Figure 4.71.

Transect Number	Cumulative crack widths (m)	Distance of first crack from river (m)
1	5.2	64
2	3.6	46
3	2.3	72



Figure 4.72: View close to river looking back towards clubhouse. Lines of ejecta are associated with lateral spreading cracks. (17 Nov 2016, S41.4881, E174.0099, facing W).



Figure 4.73: Liquefaction ejecta located 90 m east of clubhouse. (17 Nov 2016, S41.4890, E174.0105, facing E).



Figure 4.74: View of Blenheim rowing clubhouse from the north (17 Nov 2016, S41.4886, E174.0096, facing S).

The clubhouse structure at the site was a light-weight timber framed structure, with a number of timber and concrete piles visible at the rear of the structure (Figure 4.74). While ejecta were observed across large areas around the clubhouse, only minor evidence of liquefaction was observed around the perimeter of the building itself. On the western side of the building, some minor gapping (approximately 2.5 cm) was observed on the North side of a limited number of piles (Figure 4.75).

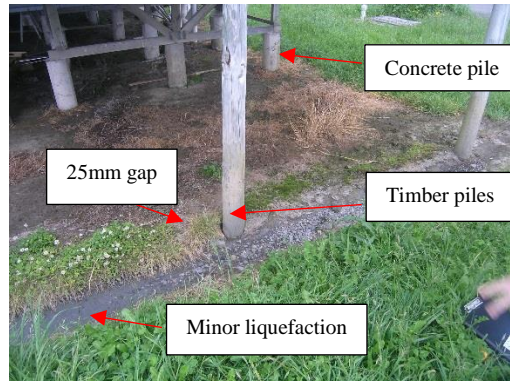


Figure 4.75: Gapping on North side of timber pile (17 Nov 2016, S41.4890, E174.0092).

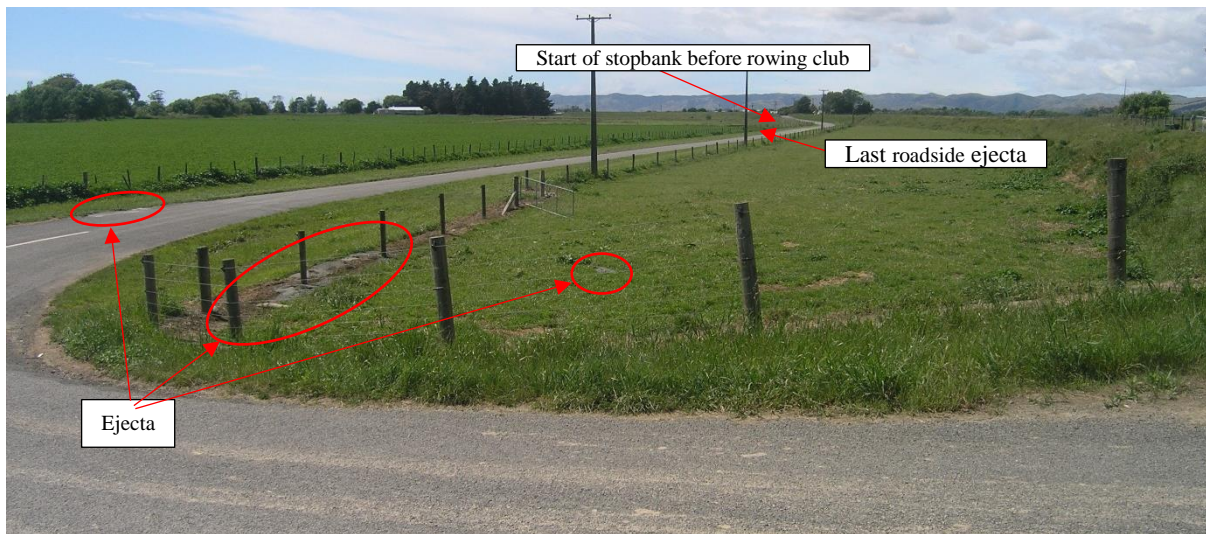


Figure 4.76: Evidence of liquefaction on approach to the Blenheim Rowing Club (17 Nov 2016, S41.4862, E174.0022, facing S).

Further back from the river, the drive-through survey first encountered sand boils 1 km to the north-west of the rowing club at the point where Jones Road crosses over the stopbank and drops onto the Wairau River terrace (highlighted in Figure 4.65 and Figure 4.76). A stopbank was present on the river side of Jones Road, starting at a distance of 500 m from the rowing club. No liquefaction manifestations were observed to the south of the embankment, nor along the roads to the east of the rowing club. The particle size distribution of a sample of ejecta taken from the location shown in Figure 4.76 is presented in Figure 4.66 and is classed as a fine sand. The gradation of this ejecta is noticeably finer than the material observed at the main Blenheim Rowing Club site.

#### 4.1.3.4 Wairau Rowing Club

The Wairau Rowing Club is located adjacent to the southern bank of the Wairau River and encompassed by the Grovetown Lagoon (Location 3 in Figure 4.51), an ox-bow lake associated with a meander bend cut off from the main channel during a flood in 1861. Satellite imagery indicates that the main channel of the Grovetown Lagoon was originally much wider than the two manmade drainage channels joining the lake with the Wairau River. The club house and launching area are located adjacent to the paleo-channel of the Wairau River. The most significant damage in this area is summarized in Figure 4.77 and is constrained between the two manmade drainage channels linking the oxbow lake to the Wairau River.

The largest lateral spreading cracks were observed in an area up to 20 m from the riverbanks, with the largest crack width being approximately 2 m. At the northern end of the grassed area to the east of the clubhouse the lateral spreading was associated with a 50 cm vertical settlement. This lateral spreading extended between the two drains linking the Wairau River and the Oxbow lake. Examples of this lateral spreading in the grassed area is shown in Figure 4.78 and near the northern drain in Figure 4.79.

A line of sand boils was located approximately parallel to the river, half way between the embankment and the river bank, and extended into the bushes immediately north of the grassed area (Figure 4.80). A 10 cm wide lateral spreading crack was observed at the northern end of this line of sand boils. A significant volume of ejecta was identified in the drainage channel between the oxbow lake and the Wairau River on the day of the earthquake (Figure 4.81a). The ejecta were quickly removed and stockpiled adjacent to the drain as shown in Figure 4.81b.

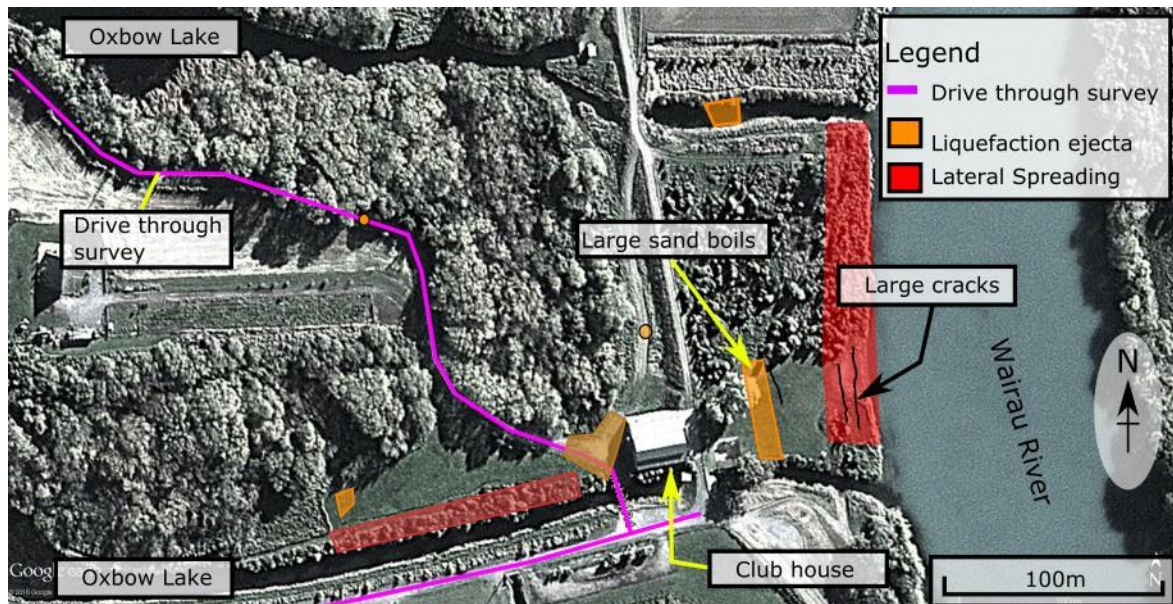


Figure 4.77: Summary of observations at Wairau Rowing Club (approx. centre of image: S41.4762, E173.9843, Imagery from GoogleEarth).



Figure 4.78: Lateral spreading cracks close to the Wairau River in the grassed area to the east of the clubhouse (17 Nov 2016, S41.4765, E173.9862, facing S).



Figure 4.79: Lateral spread crack approximately 2 m wide filled with fine grey ejecta (6 Dec 2016, S41.4761, E173.9860, facing NE).



Figure 4.80: Sand boils on lawn in front of club house shown as large sand boils in Figure 4.77 (17 Nov 2016, S41.4766, E173.9858, facing N).



Figure 4.81: a) Ejected sand evident in the drain channel (14 Nov 2016). b) Pile of excavated ejecta from the drain channel (6 Dec 2016, S41.4754, E173.9854, facing E).

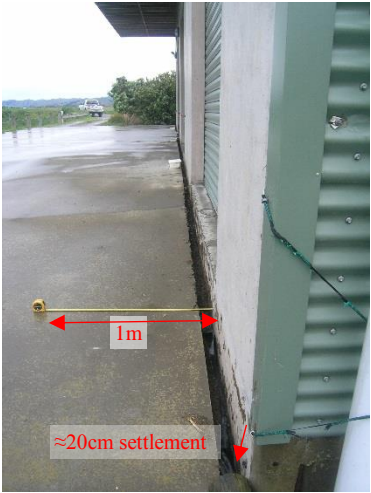


Figure 4.82: Gapping and settlement on eastern side of club house (17 Nov 2016, S41.4766, E173.9855, facing S).

The clubhouse building consists of three vertical levels and four lateral bays. The bottom level is accessible on the western side of building, while an embankment runs along the eastern side of the building with the 2<sup>nd</sup> level of the building opening out onto the top of the embankment. A 10 cm gap between the structure and the surrounding soil was apparent along the northern and eastern sides of the building. On the Eastern side in Figure 4.82, the exterior concrete slab had pulled free of the main clubhouse (attached by straight rebar), while at the north-east corner, the slab had settled 20 cm relative to the building (Figure 4.83).



Figure 4.83: Gapping and settlement on northern side of club house (17 Dec 2016, S41.4767, E173.9851, facing E).



Figure 4.84: Cracks and ejecta to the west of the Wairau Rowing Club (17 Nov 2016, S41.4768, E173.9849, facing E).

Numerous sand boils were located around the rowing club building, as well as a small number of isolated sand boils up to 200 m to the north-west on Cemetery Road. In the level area immediately to the west of the clubhouse, cracks of approximately 5 cm in width were identified, along with a number of areas of grey fine sand ejecta (Figure 4.84 and Figure 4.85) that extended parallel to the paleo-channel comprising the oxbow lake as shown in Figure 4.77.



Figure 4.85: Fine grey sand ejecta west of the Wairau Rowing Club (7 Dec 2016, S41.4771, E173.9836, facing E).

#### ***4.1.4 Lower Opaoa River***

Downstream of the Blenheim urban area there was significant lateral spreading and large volumes of ejecta were observed along the inner banks of the meander bends of the Lower Opaoa River. Figure 4.86 provides a summary of the damage observed from ground and aerial reconnaissance.

There was damage to the stopbank network in four locations along this stretch of the river as shown in Figure 4.86. The main impact was to wineries situated along the river, with large areas of vines affected as indicated in Figure 4.87 and Figure 4.88. Many of these areas were rapidly cleared following the earthquake, and new end-posts were installed to allow the rest of the vines to continue to grow.

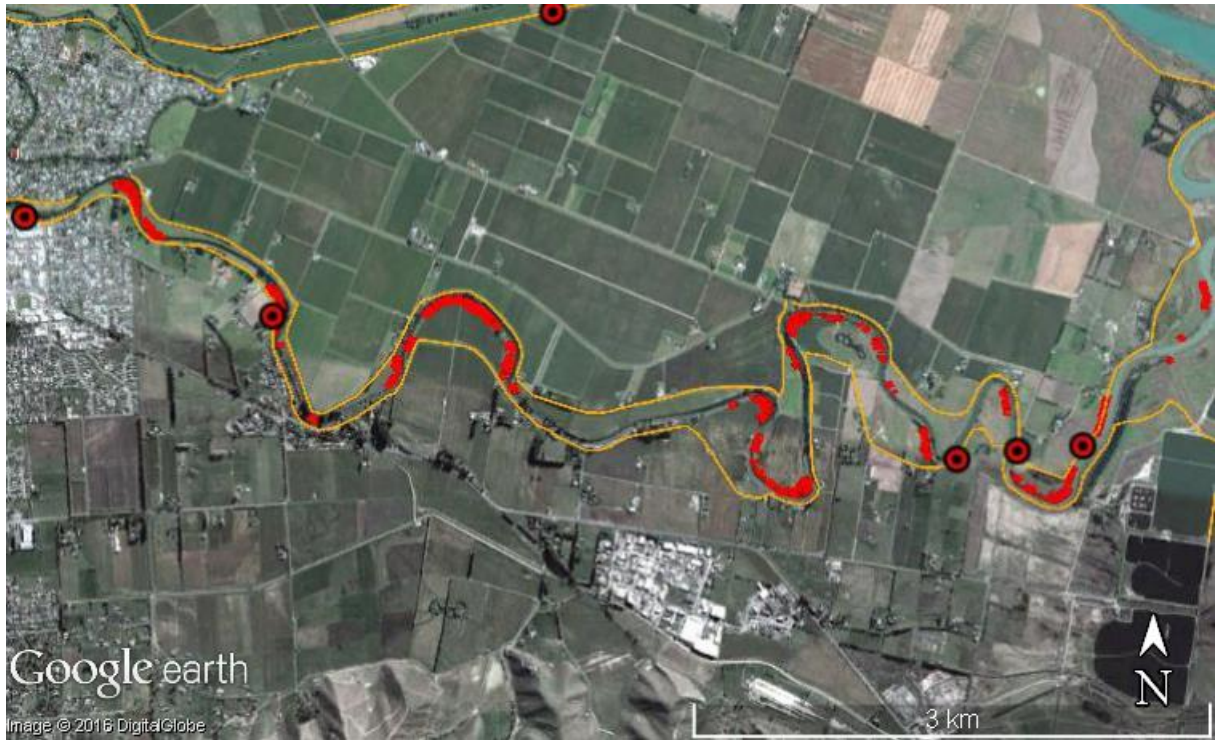


Figure 4.86: Summary of damage along the Lower Opaoa River. Red areas indicate locations of cracking and ejecta, with stopbank damage shown by the red symbols in this figure. Orange lines indicate locations of stopbanks. (Approx. centre of image: S41.5219, E174.0076, Imagery from GoogleEarth).



Figure 4.87: Lateral spreading and sand ejecta damage to vineyards along the Lower Opaoa River. Photo taken 4 days after the earthquake showing vine repair yet to commence (18 Nov 2016, S41.5217, E174.0160, facing W, Marlborough District Council 2016).



Figure 4.88: Lateral spreading and sand ejecta damage to vineyards along the Lower Opaoa River. Photo taken 4 days after the earthquake showing completed vine repair and remnants of damaged vines. (18 Nov 2016, S41.5270, E174.0179, facing N, Marlborough District Council 2016).

#### ***4.1.5 Opaoa and Omaka River (upstream of Blenheim)***

Upstream from the Blenheim urban area (starting at Lansdowne Park) there was evidence of minor liquefaction, but it did not have any significant effect on the built environment. Ejecta were observed at the side of O'Dwyers Road as indicated in Figure 4.89, between 85 and 65 m from the crossing over the Opaoa River. Ejecta closest to the river were brown in colour, while it became grey in color moving away from the river. At this location, a small tributary stream runs parallel to the road, 15 m to the East.

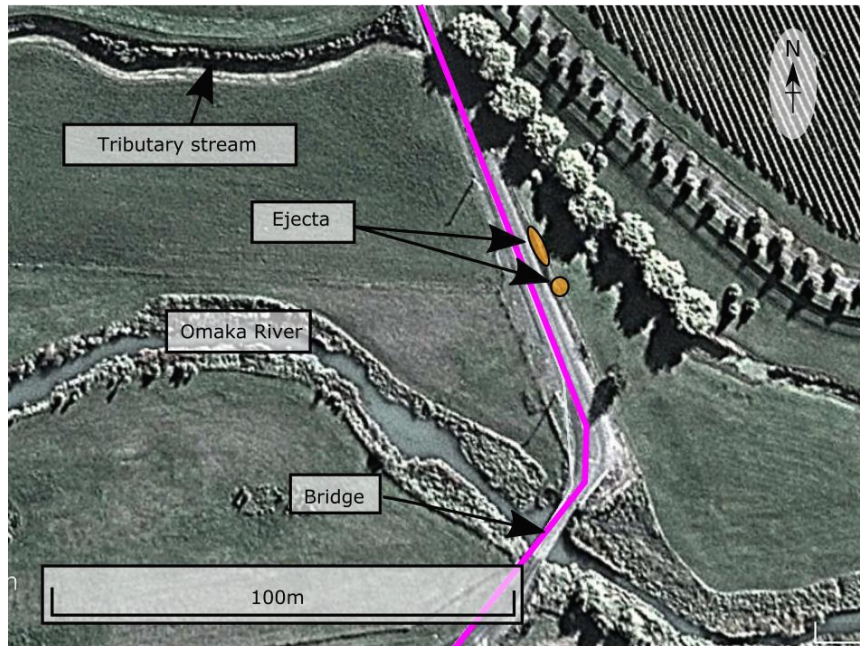


Figure 4.89: Summary of observations at O’Dwyers Road/Thomsons Ford Road bridge (approx. centre of image: S41.4825, E173.9336, Imagery from GoogleEarth).



(a)



(b)

Figure 4.90: Sand boils at O’Dwyers Road. (a) facing SE (b) facing NW (17 Nov 2016, S41.4822, E173.9340).

#### 4.1.6 Greater Marlborough Area

Outside of the Wairau Plain and Blenheim, reconnaissance moved south along State Highway 1 towards the town of Ward. The main liquefaction related impacts were associated with bridge damage. A more complete summary of the liquefaction related impacts to bridges is provided in Chapter 6.

## 4.2 Overview of Kaikoura Reconnaissance

The town of Kaikoura is located on the east coast of the South Island of New Zealand, approximately 160 km NNE of Christchurch and 100km SSE of Blenheim. The urban area of Kaikoura covers an area of approximately 7 km<sup>2</sup> and has population of around 2000, with an additional 2000 people living in the nearby rural areas at the time of the 2013 census (Statistics NZ, 2013). The township is mainly concentrated in a thin band extending 500 m inland from the coast. Before the earthquake, the economy of Kaikoura was focused on tourist activities, as well as agriculture on the coastal plains. Following the earthquake, all roads to Kaikoura were impassable as a result of the many landslides in the area. Initial evacuations took place by sea and air (helicopters) until partial road access was restored on the 18<sup>th</sup> November 2016.

Members of the GEER reconnaissance team were able to briefly visit Kaikoura with assistance from the local consulting firm Tonkin + Taylor Ltd. (T+T) between 8<sup>th</sup> and 10<sup>th</sup> December 2016. T+T engineers had been conducting damage surveys on behalf of the New Zealand Earthquake Commission (EQC); photographs collected during their efforts in Kaikoura have been included within this section of the report.

There is one strong motion station in the Kaikoura area, located on the rocky Kaikoura Peninsula to the south of town (Site Class B according to NZS1170.5, SNZ 2004). During the main earthquake event, PGAs of 0.22 g (horizontal geometric mean) and 0.27g (vertical) were recorded. Several aftershocks occurred within 24 hours, including 3 events with  $M_w$  greater than 6 with nominal epicenters within 35 km of Kaikoura. However, accelerations during the main shock were significantly larger than the aftershocks which had horizontal PGAs less than 0.1 g. It is assumed that the damage sustained in Kaikoura arose as a result of the main earthquake, though significant excess pore pressures may have remained at the time of the aftershocks.

The area covered by the overall reconnaissance efforts is shown in Figure 4. along with key locations where damage was observed. Due to the rural nature of this area, the damage to infrastructure was quite low. Damage was concentrated along Lyell Creek, where large lateral displacements were observed within 30 m of the creek resulting in heavy damage to many houses built close to the river, and to one short-span bridge (see Chapter 6 of this report). While these displacements resulted in cumulative crack widths of up to 3 m, it was apparent that the driving mechanism was not due to classic liquefaction-induced lateral spreading, as discussed subsequently. Other damage in the region included cracking and deformation of the roads, as well as some damage to the liner systems in embankments at the oxidation ponds to the north of the town. Liquefaction ejecta was noted in some areas outside of the main township, though the overall impact of liquefaction was quite small.

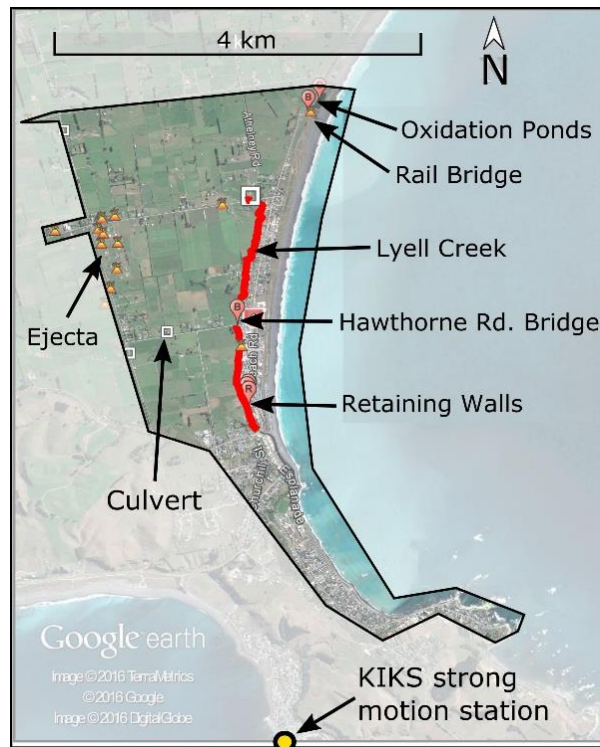


Figure 4.91: Reconnaissance in Kaikoura (approx. centre of image: S42.389, E173.682).

#### 4.2.1 Geology of the Kaikoura Area

The township of Kaikoura is situated within a highly tectonically and geomorphically active region along the eastern coast of New Zealand's South Island. The region is located at the eastern-most extent of the north-east trending strike-slip transpressive Hope Fault. Uplift along the Hope Fault results in the northeast-trending Seaward Kaikoura range located to the west of the township. The Hope Fault is currently the most active structure of the Marlborough Fault System with a right-lateral slip rate of 20–40 mm/year (see Chapter 2; Cowan 1991; Van Dissen & Yeats 1991).

The town centre is situated proximal to the coast and upon uplifted beach deposits and alluvial out-wash fans of the braided Kowhai and Hapuku Rivers which flow eastward from the Seaward Kaikoura Range. The region is predominantly underlain by alluvial gravels with interspersed sands deposited by the braided rivers which avulsed across the region. These alluvial sands are cross-cut by channels and associated flood deposits of smaller streams. Late Quaternary displacements on the Hope Fault have offset the watershed of the Kowhai River, which combined with likely co-seismic aggradation, have resulted in channel avulsion across the region. The alluvial sediments within ~500 m of the coast are inter-fingered with coastal gravels and sands associated with historical coastlines. The maximum inland extent of the coastal sediments is likely reflected by Lyell Creek running along the western most extent of the township, and tectonic uplift of the region combined with marine regression following the mid-Holocene high-stand. The loosely consolidated nature of the flood deposits from the small streams within the township, combined with shallow water-tables (1 to 2-m depth)

poses a localized high liquefaction hazard for the region. Localized pockets of beach sand within the gravels are also potentially liquefiable.

The southeast section of the township is located upon the Kaikoura Peninsula and associated bays. The peninsula is comprised of a flight of uplifted and folded marine terraces underlain by a Late Cretaceous-Paleogene Siltstone and Limestone succession that unconformably overlies Torlesse greywacke. The rocks comprising the peninsula are folded on kilometre scale wave lengths reflecting crustal shortening on multiple, southeast-facing thrust faults present both on land and continuing offshore. Paleo-sea-cliffs and uplifted beach deposits surround the base of the Peninsula and provide a high rockfall and landslide hazard for the settlement.

#### 4.2.2 Liquefaction in and around Kaikoura

Liquefaction was observed in a limited number of locations in the Kaikoura area, with most located along Mt Fyffe Road and along Lyell Creek which runs parallel to and just west of Beach Rd (shown in Figure 4.). The locations where liquefaction ejecta was observed are shown in Figure 4.92. In each case, the amount of ejecta was considered minor to moderate; examples of the ejecta features observed are shown in Figure 4.93 to Figure 4.98. Surface colouring visible in aerial photography of the area (courtesy LINZ) suggests that these ejecta could be associated with paleo channels of the Kowhai River, which currently reaches the sea to the south of Kaikoura. Samples of ejecta material were recovered from two locations, marked as “SR-1” and “BR-1” in Figure 4.92; the first from a sand boil at the roadside on Schoolhouse Road (Figure 4.93), and the second from an area of intense cracking along Lyell Creek, behind Beach Road (Figure 4.94). Figure 4.93 (b) shows the particle size distributions of these samples, which were obtained by wet sieving. Laboratory testing confirmed that both samples were non-plastic.

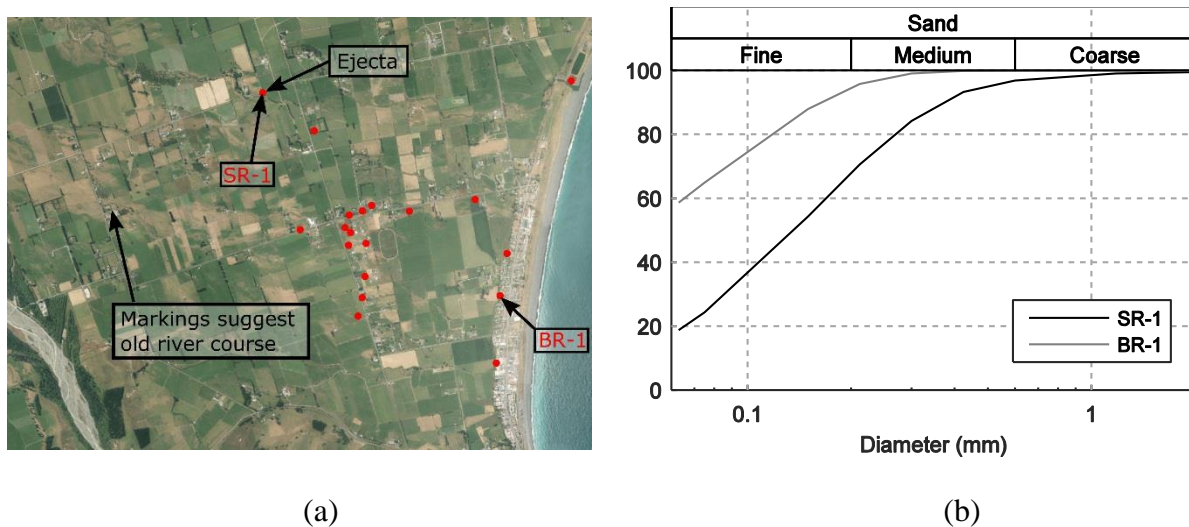


Figure 4.92: (a) Locations of observed liquefaction ejecta; SR-1 and BR-1 refer to locations where ejecta samples were obtained (approx. centre of image: S42.375, E173.647). (b) Particle size distribution of the samples SR-1 and BR-1.



Figure 4.93: Liquefaction ejecta on Schoolhouse Road where sample SR-1 was taken (-9 Dec 2016, S42.3681, E173.6496, facing SE).



Figure 4.94: Liquefaction ejecta in the bank of Lyell Creek inland of Beach Road where ejecta sample BR-1 was obtained. Note the light colour of the material (-9 Dec 2016, S42.3916, E173.6777, facing E).



Figure 4.95: Liquefaction in a vegetable patch on Mt Fyffe Road. Note the ejecta issued from ground cracks (-date to be added in V2.0 of report, S42.3813, E173.6622, facing S).



Figure 4.96: Liquefaction in driveway on Mt Fyffe Road (- date to be added in V2.0 of report, S42.3800, E173.6600).



Figure 4.97: Ejecta in the field 50 m west of Mt Fyffe Road (– date to be added in V2.0 of report, S42.3877, E173.6610).



Figure 4.98: Liquefaction ejecta in the field south of Mill Road. Note: the ejecta is concentrated in lines which continue in the background over a total length of 100 m (– date to be added in V2.0 of report, S42.3772, E173.6753, facing SE).



Figure 4.99: Front area of house on Schoolhouse Road (–9 Dec 2016, S42.3680, E173.6500, facing SW).

On Schoolhouse Road north of Mt Fyffe Road (Figure 4.93 and Figure 4.99), a structure had visibly settled, with markings on a wastewater vent pipe suggesting the settlement on the eastern side of the house was approximately 6 cm (Figure 4.100). Misalignment of a drainpipe with its associated drain shown in Figure 4.101 indicates that the house had also moved 10 cm parallel to its major plan axis (SSE) relative to the ground. Additionally, a vertical gap up to 20 cm wide was present on the eastern side of the house. The combined settlement and lateral movement of the house resulted in cracking of the unreinforced block (Figure 4.102). On the front lawn of the structure, a 5 cm ground crack appeared to follow the line of buried services to the road (Figure 4.100).



Figure 4.100: View of east wall of house on Schoolhouse Road (-9 Dec 2016, S42.3682, E173.6501, facing S).



Figure 4.101: Misalignment of drain pipe and drain on east side of house on Schoolhouse Road (-9 Dec 2016, S42.3683, E173.6501).



Figure 4.102: Cracking through brick work on SW corner of house on Schoolhouse Road (-9 Dec 2016, S42.3684, E173.6501, facing W).



Figure 4.103: Damage caused to house on Mill Road by lateral ground movements (- date to be added in V2.0 of report, S42.3784, E173.6675, facing NE)

A number of sand boils were observed around the intersection of Mt Fyffe and Mill Road, minor to moderate in size. At a house on Mill Road, damage to the structure shown in Figure 4.103 was caused by an outdoor concrete slab displacing laterally to the north relative to the house (Figure 4.104). Also, a newly built house located on Mt Fyffe Road experienced some settlement, and vertical gaps up to 10 cm wide had formed at some places around the perimeter (Figure 4.105). In front of the house, a buried septic tank had floated approximately 30 cm relative to the ground (Figure 4.106). While no obvious ejecta were observed at the house, small sand boils were discovered in the fields approximately 50 m west of the house (Figure 4.97).



Figure 4.104: Separation of outdoor slab from main foundation slab (date to be added in V2.0 of report, S42.3784, E173.6675, facing E)



Figure 4.105: Southern side of new house on Mt Fyffe Road (8 Dec 2016, S42.3877, E173.6620, facing W).



Figure 4.106: Floation of septic tank at SE corner of house on Mt Fyffe Road (8 Dec 2016, S42.3876, E173.6621, facing N).

### 4.2.3 Lateral Displacements and Ground Failure

Many instances of lateral ground movement were observed on the banks of the creeks and drainage ditches in the Kaikoura area. The most significant impacts to infrastructure, as well as some of the most severe lateral displacements and/or ground failures, occurred along an ~2 km stretch of Lyell creek which forms the western boundary of the heavily developed region of Kaikoura, as shown in Figure 4.107.

Ground cracks were observed on both sides of Lyell creek, with the lateral displacements varying significantly in magnitude. Some of the largest displacements were located between and 140 and 190 Beach Road (including Gillings Lane) where displacements in excess of 2.5 m occurred within 30 m of the creek in a few locations, while cumulative displacements in the range of 0.5 – 2 m were common elsewhere. A selection of photographs showing some of the lateral displacements and their effects on the residential buildings in this area are shown in Figure 4.109 to Figure 4.122. It was also noticeable that at a number of locations, the cracks were also associated with large vertical offsets, with the soil blocks rotating with their bases moving inwards towards the river relative to their tops; Figure 4.111 and Figure 4.120 show two examples of this. This deformation mechanism may imply the occurrence of cyclic softening and deeper seated slumps, rather than solely lateral spreading



Figure 4.107: Lyell Creek and locations of photographs of interest (for reference the coordinates of 4 Gillings Ln are S42.3841, E173.6786).

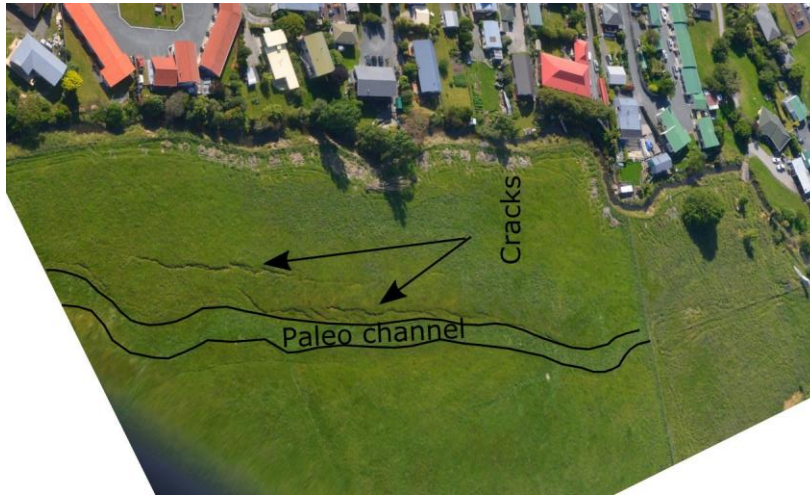


Figure 4.108: Lateral displacement associated with a paleo channel (approx. centre of image: S42.3808, E173.6787).



(a)



(b)

Figure 4.109: Separation of concrete slabs and garage (70 cm wide) due to lateral ground movements towards Lyell Creek (date to be added in V2.0 of report,): (a) S42.3822, E173.6801; (b) S42.3821, E173.6802. Note the garage has moved laterally in the picture (i.e. Lyell Creek is behind the garage, to the left of the picture).



Figure 4.110: Lateral displacements (approx. 1.5 m in total) caused a loss of support at the NW corner of a house on Beach Road, causing cracking in the brick wall (date to be added in V2.0 of report, S42.3823, E173.6800).



Figure 4.111: Large vertical offset (50 cm) associated with the ground movement north of Gillings Lane (– date to be added in V2.0 of report, S42.3841, E173.6784).



Figure 4.112: Lateral displacements with large vertical offsets at Gillings Lane (– date to be added in V2.0 of report, S42.3841, E173.6784).



Figure 4.113: Floatation of manhole on Beach Road near to Lyell Creek (– date to be added in V2.0 of report, S42.3848, E173.6783).



(a)



(b)



(c)

Figure 4.114: Complete loss of support to foundations at west end of house on Beach Road (– date to be added in V2.0 of report, S42.3851, E173.6783).



(a)



(b)

Figure 4.115: Lateral ground movement caused separation of two semi-detached houses on Beach Road (– date to be added in V2.0 of report, S42.3857, E173.6783).



Figure 4.116: Cracks running through the house closer to Lyell Creek (– date to be added in V2.0 of report, S42.3857, E173.6783).



Figure 4.117: Gapping at the west side of the house closer to Lyell Creek (date to be added in V2.0 of report, S42.3857, E173.6783).



(a)



(b)

Figure 28: A garage/shed at a house on Beach Road displaced approx. 1 m towards the Lyell Creek, and moved downwards approx. 1 m (– date to be added in V2.0 of report, S42.3860, E173.3860).



Figure 4.118: Lateral displacement with vertical offsets close to Hawthorne Road Bridge (– date to be added in V2.0 of report, S42.3885, E173.6776).



(a)



(b)

Figure 4.119: Lateral movement south of Hawthorne Road Bridge (– date to be added in V2.0 of report, S42.3894, E173.6775).



Figure 4.120: Lateral displacements at 105 Beach Road. Note: Cracks are associated with vertical offsets and blocks have rotated away from the river (i.e., slumped) (9 Dec 2016, S42.3902, E173.6777).



(a)



(b)

Figure 4.121: Cracks in footpath between 105 and 73 Beach Road, running east of and parallel to Lyell Creek. Largest crack in footpath (right hand photo) was 1 m wide and 70 cm deep (9 Dec 2016): –(a) S42.3916, E173.6778; (b) S42.3926, S173.6777.



Figure 4.122: Lateral displacement at 87 Beach Road 13 m east of Lyell Creek (date to be added in V2.0 of report, S42.3917, E173.6778).



Figure 4.123: Recent earthworks on west side of Lyell Creek, opposite 87 Beach Road. (9 December 2016, S42.3922, E173.6777).

No foot surveys were carried out on the western side of the creek; however, some cracks were visible from the eastern bank and in aerial photographs. Figure 4.108 shows a pair of large lateral spreading cracks which were spotted during a helicopter flight. These cracks are approximately 50 m west of Lyell Creek, significantly further than the majority of other cracks. Inspection of aerial photographs indicates that these cracks are likely to be associated with the paleo channel marked in Figure 4.107.

It is expected that there were many cracks that were not observed as a result of the heavy vegetation obscuring individual cracks. Additionally, at the time of the visit on the 9<sup>th</sup> December 2016, recent earthworks were visible on the western bank of the creek (shown in Figure 4.123) , which are assumed to indicate that some bank stabilization or dredging of the creek was carried out soon after the earthquake.

Detailed transects were carried out at three locations along Beach Road following the approach used by Robinson et al. (2011), as shown in Figure 4.124. At each location, individual crack widths, distance from the river channel, and the change in vertical elevation were measured using a tape measure and a range finder. Additionally, the height of the free-face, determined using a tape measure, was used to estimate the difference in height between the bank and the base of the river channel directly next to the start of the transect. The red

lines in the figure indicate the zone of significant cracking. The data from these transects (summarised in Table 4.3) indicate that the lateral displacements in these locations were in the range of 0.6 to 1.1 m, while cracking was typically concentrated within 15 m of the river channel.

Despite the large lateral movements, ejecta were not widespread on the east side of Lyell Creek, with only relatively small sand boils (~50 cm diameter) being observed at a few locations along Beach Road (visible in Figure 4.94).



Figure 4.124: Location of transects (approx. centre of image: . S42.3922, E173.6791).

Table 4.3: Summary of transects along Lyell Creek

Transect Number	Cumulative crack width (m)	Max distance of crack from creek (m)	Creek depth (m)
1	1.12	7.3	0.3
2	0.62	15.0	0.7
3	0.96	13.3	1.0

## 4.2.4 Impacts on Infrastructure & Structures

### 4.2.4.1 Oxidation Ponds

Kaikoura's waste water is treated at a facility located north of the main town adjacent to the railway line, and immediately south of School House Road. Between March 2015 and March 2016, the total discharge from the ponds was approximately 320,000 m<sup>3</sup>, an average of 880 m<sup>3</sup> per day (KDC 2016). At its southern end, the facility is bordered by Middle Creek, while beach exists to the east. On both the southern and eastern sides, the land slopes steeply to the level of the current river and the beach respectively. An overview of the site is shown in Figure 4.125, and for the purposes of this section, the northern and southern ponds are referred to as KK-OPN and KK-OPS.

This facility was inspected by Tonkin +Taylor engineers following the earthquake on the 22<sup>nd</sup> November 2016. At the time of inspection, KK-OPS had been fully drained. Lateral spreading cracks were present on the river side of the bank at the south end of the pond (Figure 4.126) while liquefaction ejecta were also present on the river terrace close to one of the piers of the railway bridge (discussed in Chapter 6). Deformations were visible along the crest of the pond, particularly at the most westerly corners, where significant settlement was visible (Figure 4.127 to Figure 4.129). The deformation at these corners was sufficient to cause tearing in the pond's geo-liner, shown in Figure 4.127. Significant settlement was also evident on the eastern side, and a second major tear in the geo-liner was present close to a number of transverse cracks in the bank (Figure 4.128). A concrete slab supporting a vent pipe was completely exposed by the settlement of the ground (Figure 4.131). Aeration lines were strung between posts on the north and south edges of the pond. These posts rotated significantly, particularly on the south edge of the pond (Figure 4.132).

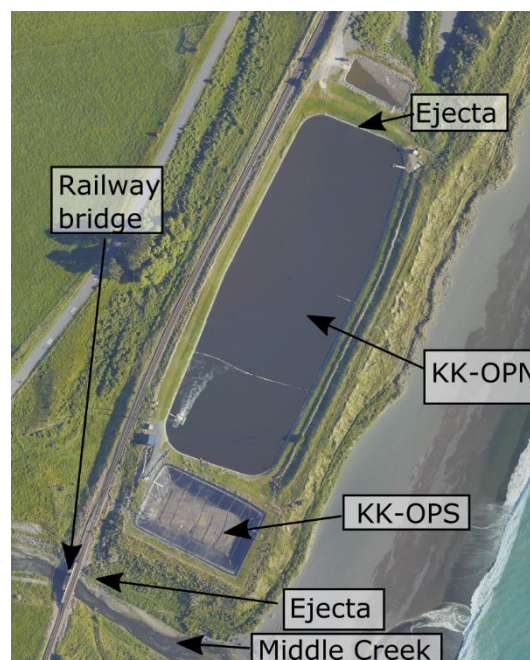


Figure 4.125: Overview of Oxidation Ponds north of Kaikoura (approx. centre of image: S42.366, E173.687). (modified from LINZ, 2016)



Figure 4.126: Lateral spreading in the bank on south edge of oxidation ponds (– date to be added in V2.0 of report,, S42.3672, E173.6866, facing W.)



Figure 4.127: KK-OPS looking from the SW corner. Note: geo-liner in the foreground has ripped (– date to be added in V2.0 of report,, S42.3668, E173.6865, facing E).



Figure 4.128: KK-OPS from eastern edge. Note geo-liner is ripped in foreground and uneven settlement on the west side is visible in the background (– date to be added in V2.0 of report, S42.3669, E173.6874, facing W).



Figure 4.129: West edge of KK-OPS. Large differential settlements of the crest are visible (– date to be added in V2.0 of report, S42.3668, E173.6865, facing N).



Figure 4.130: East side of KK-OPS. Note ripped geo-liner in line with crack by third post from left (– date to be added in V2.0 of report, S42.3667, E173.6875, facing SE).



Figure 4.131: Protruding vent pipe on east edge of KK-OPS due to ground settlement (– date to be added in V2.0 of report, S42.3668, E173.6875, facing S).

The larger oxidation pond (KK-OPN) was still full at the time of the inspection, however, transverse cracks in the concrete lining were visible (Figure 4.133). Figure 4.134 shows a section of concrete lining which had moved laterally towards the centre of the pond near the SW corner of KK-OPN. In addition to this movement, general lateral movement of the ground towards the pond was highlighted by gapping around a metal anchor rod at the edge of the pond.



Figure 4.132: Rotation of the aeration-line control posts on the south side of KK-OPS (– date to be added in V2.0 of report, S42.3669, E173.6867, facing E).



Figure 4.133: North edge of KK-OPN. Note cracking and overlayering of concrete. Ejecta visible on concrete. (– date to be added in V2.0 of report, S42.3647, E173.6884, facing W).



Figure 4.134: West edge of KK-OPN. Note concrete panel has displaced into pond (– date to be added in V2.0 of report, S42.3660, E173.6868, facing N).

#### 4.2.4.2 Retaining Walls

Several properties to the east of Lyell Creek had constructed wooden retaining walls. At 87 Beach Road, a 2 m tall wooden retaining wall had been built at approximately 70 m west of Lyell Creek and appeared to have performed well with no signs of lateral displacement (Figure 4.135). However, at 29, 33, and 35 Beach Road, the retaining walls showed signs of failure.

On Beach Road, a retaining wall had been built at the rear of a long motel building. The timber retaining wall was constructed approximately 12 m from Lyell creek, on a section of raised ground, which is visible in Figure 4.136. The crest of the retaining wall had moved 30-40 cm towards the river, based on gaps which had opened up between the concrete slab and the fence on the retained side of the wall.

A second retaining wall on Beach Road is located roughly 30 m east of Lyell Creek. Figure 4.138 shows this retaining wall, where the top of the retaining wall had bulged 20-30 cm towards the creek. Cracks of up to 5 cm wide were present in the concrete slab approximately 5 m back from the top of the wall and are visible in Figure 4.139.



(a)



(b)

Figure 4.135: Good performance of retaining wall at 87 Beach Road (–9 Dec 2016, S42.3917, E173.6785: (a) facing E; (b) facing SE.



Figure 4.136: Failure of retaining wall (– date to be added in V2.0 of report, S42.3973, E173.6798, facing N).



Figure 4.137: Cracks behind retaining wall (– date to be added in V2.0 of report, S42.3971, E173.6798, facing N).



Figure 4.138: Failure of retaining wall (– date to be added in V2.0 of report, S42.3964, E173.6793, facing N). Note: Cracks visible in the car park on the retained side of the wall.



Figure 4.139: Cracks visible behind retaining wall (– date to be added in V2.0 of report, S42.3968, E173.6796, facing S).

### 4.3 Summary of Reconnaissance Amuri and Emu Plains

The Amuri and Emu Plains (lying south and north of the Waiau River, respectively) comprise the relatively flat bottomed Waiau valley in North Canterbury bounded to the north by the Amuri Mountain range and the Lowry Mountain range to the south and east. The area is rural, with two minor towns (Rotherham and Waiau) located towards the north-east of the valley. Waiau is the larger of the towns and has a population of ~260 (Statistics NZ, 2013) and is located at the confluence of the braided Waiau and Mason Rivers. Additional townships are located within this valley, but they are similarly small in population.

The township of Waiau is built upon alluvial fill sequences, predominantly comprised of gravels, associated with Pleistocene glaciation and the subsequent outwash surface, and the later development of the Waiau River (Rother, 1996). Much of the overbank flood-plain surrounding the Waiau River is used as farmland and is underlain by alluvial gravels with localised sand lenses and capped by over-bank silts. Smaller active and paleo-stream channels are present within the flood plain, along with paleo-channels of the Waiau River which are recognizable as topographic depressions within the farmland. The active and paleo-channels are likely comprised of alluvial gravels and sands.

The sequence of fault ruptures associated with the Kaikoura earthquake began relatively close to the township of Waiau and propagated in a north-easterly direction. The WTMC strong motion station, located approximately 4 km north of Waiau town (position marked in Figure 4.), indicated that this region experienced extremely strong shaking, with horizontal accelerations in excess of 1 g, and vertical accelerations of 2.7 g. Evidence of the strong ground motions in this regions included broken wooden power pylons (observed in Waiau and along River Road), clear displacement of large stone blocks in Waiau, and the toppling of gravestones in the town of Rotherham.

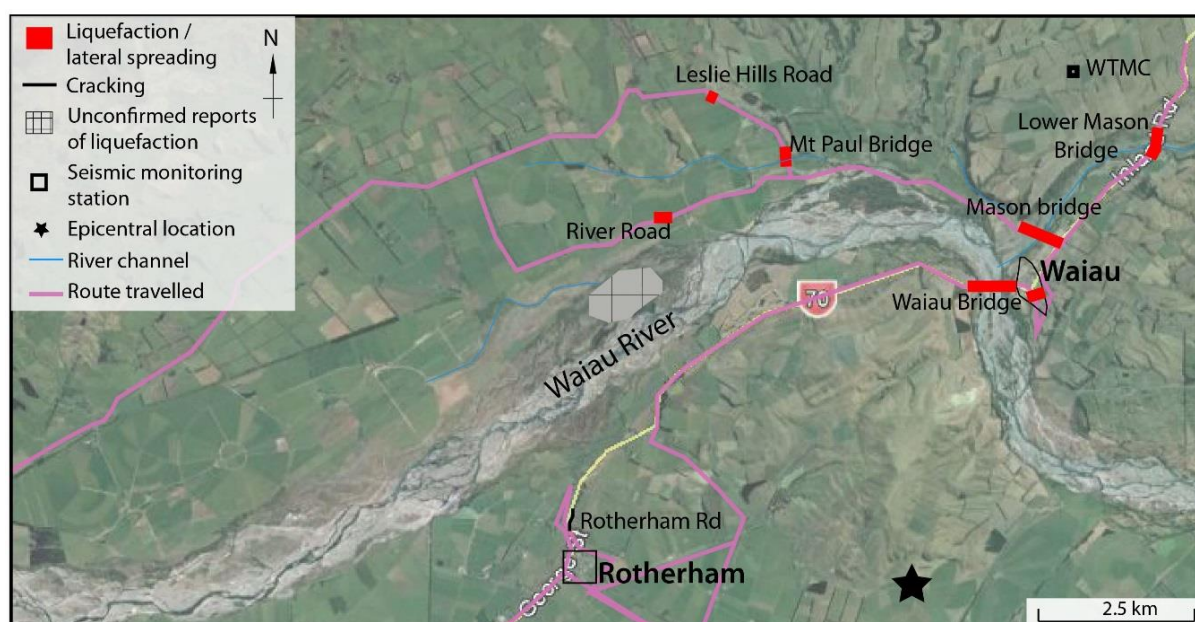


Figure 4.140: Map of the Waiau area indicating areas with liquefaction manifestation. (approx. centre of image: S42.658, E173.005).

Reconnaissance in this area was undertaken relatively soon after the earthquake, with the first exploratory visit to the region taking place on the 15 Nov 2016. Additional visits occurred on the 17 and 18 Nov 2016. The extent of damage in this area was not well-known immediately, and the reconnaissance on the 15 Nov 2016 aimed only to see as much as possible to assess the levels of earthquake related damage. The additional trips on the 17 and 18 Nov aimed to visit the town of Waiau and the surrounding bridges. Most of the reconnaissance in these regions involved drive-through surveys, because it was not logistically possible to carry out reconnaissance in most areas away from the main roads. The routes covered during the reconnaissance are shown in Figure 4..

Damage to buildings and infrastructure in this region was largely caused by the high inertial loads. Due to the sparse population in the area, the building stock is largely single storey, light residential buildings, and there were damaged brick facades, fallen chimneys and damage to unreinforced masonry walls throughout the town of Waiau. The main impacts to infrastructure in the region were to the multi-span bridges crossing the Waiau, Mason, and Wandle Rivers, where the inertial loading caused severe structural damage. These bridges are discussed in Chapter 6 of this report and by Palermo et al. (2017). Common geotechnical issues included settlement and outward cracking of the approaches, while abutment rotation and cracking was observed at a small number of bridges. Liquefaction was observed in some locations but was generally not widespread in the surveyed areas. Major liquefaction-induced lateral spreading was not observed by the reconnaissance teams in this region, though it may have contributed to some of the bridge abutment damage and road cracking.

It is important to state that surface expressions of fault rupture were present in the region, and in particular, part of the rural Leslie Hills Road was completely destroyed by a rupture transverse to the road. In this same area, there were both tension cracks and compressional features, the latter of which was made obvious by sagging fence lines and by ridges in the road surface. Further information on the observations made at this site are provided in Chapter 6.

### 4.3.1 Rotherham

Despite the strong shaking in Rotherham, no evidence of liquefaction was observed in the town. North of Rotherham, cracking both in the road and on the road sides were observed as shown in Figure 4.141 and Figure 4.142, and are representative of damage in the area (noting that the area was more severely affected by landslides).



Figure 4.141: Cracks alongside Rotherham road (S42.6908, E172.9470, 17 Nov 2016).



Figure 4.142: Large crack in middle of roadway on Rotherham Road. Crack width 20-30 cm. Vertical offset is approximately 4 cm (S42.6900, E173.9462, 17 Nov 2016).

### 4.3.2 Waiau

In the town of Waiau, the strong shaking caused damage to a large number of building facades and chimneys (examples are shown in Figure 4.143), however there was only evidence of liquefaction at two locations at the south end of the town. In this part of town, there were a number of cracks in the road, and the two locations of ejecta were either associated with the cracks (Figure 4.144), or with fence posts which surrounded a paddock SW of the end of Parnassus Street. The particle size distribution of a sample of this ejecta is shown in Figure 4.145. It was reported by utility workmen that there was a significant amount of ejecta inside the paddock, but the owner could not be located to obtain access to this area.



(a)



(b)

Figure 4.143: Damage to houses in Waiau. (a) fallen chimney (b) damage to façade. (S42.66, E173.04, 17 Nov 2016)

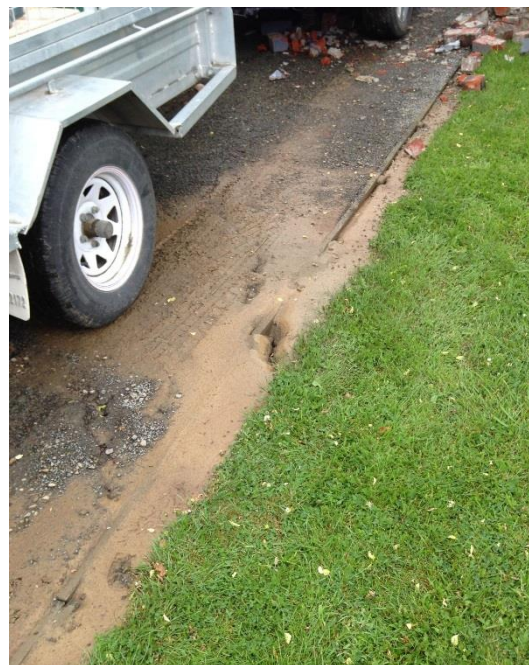


Figure 4.144: Liquefaction at the south of Waiau town (date to be added in V2.0 of report, S42.6592, E173.0440, 17 Nov 2016).

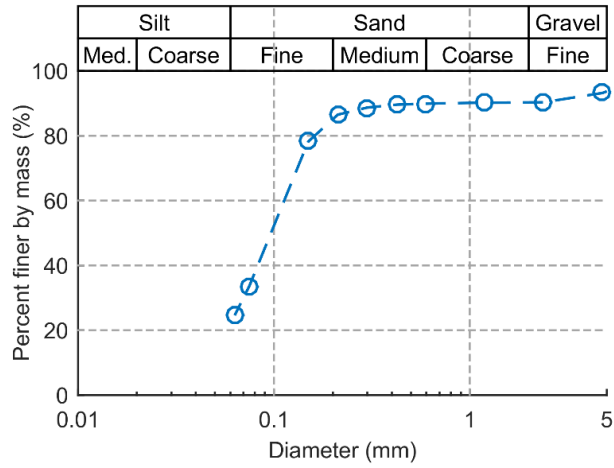


Figure 4.145: Particle size distribution of liquefaction ejecta in Waiiau town



Figure 4.146: Standing water and ejecta west of Waiiau town (date to be added in V2.0 of report, S42.638, E172.993).



Figure 4.147: Liquefaction ejecta on River Road (S42.6427, E172.9743, 17 Nov 2016).

Liquefaction was observed in the agricultural areas close to the Waiau River, west of Waiau town. Aerial photography of this area (Figure 4.146) shows standing water and ejecta in the fields as well as on the roads. The presence of sand boils in this area was confirmed by ground teams, who noted the presence of a number of ground cracks in the same area.

#### 4.4 Greater Christchurch Urban Area

The greater Christchurch area is located south of the fault ruptures associated with the Kaikoura earthquake on the eastern coast of the South Island and experienced relatively low peak ground accelerations, with the largest recordings showing around 0.08 g in Kaiapoi and 0.04 g within Christchurch itself. The low peak accelerations recorded at the strong motion stations within Christchurch and were considered unlikely to cause any significant impact. However, given the repeated liquefaction during the larger shocks of the 2010–2011 Canterbury Earthquake Sequence, as well as relatively minor events such as the 2016 Valentine’s Day earthquake when there were relatively low levels of shaking, it was decided to investigate whether there were any signs of fresh liquefaction at sites which had displayed particularly low liquefaction resistance in the past.

Four sites were selected for this purpose as shown in Figure 4.148: Swindells Road in Waikuku Beach (S42.2839, E172.7180); Cassia Place in Kaiapoi (S43.3851, E172.6704); Atlantis Street in New Brighton (S43.4956, E172.7038); and Seabreeze Close in Bexley (S42.5184, E172.7203). There was no indication that liquefaction triggered during the 2016 Kaikoura earthquake at any of these sites, and on this basis the decision was taken not to carry out any additional reconnaissance. Isolated cases of minor liquefaction were reported, and others may have gone unnoticed and unreported, but the impacts of these features on infrastructure were negligible



Figure 4.148: Locations of potential liquefaction sites in and around Christchurch (approx. centre of image: S43.417, E172.647).

## 4.5 Summary

The  $M_w 7.8$  Kaikoura earthquake involved the rupture of multiple faults in the Marlborough Fault Zone and caused widespread disruption in the north-east region of the South Island of New Zealand. Despite the large magnitude of the earthquake and high ground accelerations, relatively limited liquefaction and ground damage were observed in the Waiau Valley (where ground motions were strongest) and in the townships of Blenheim and Kaikoura.

Severe manifestations of liquefaction and lateral spreading were observed within the floodplains of the Lower Wairau and Opaoa Rivers in the area the north and east of Blenheim township. Few structures exist in this area, and hence the immediate impact on infrastructure was negligible. The locations worst affected correspond with abandoned channels or inner meander bends of the rivers. Stopbank damage occurred in locations where they crossed younger deposits in paleo channels and exhibited heavy cracking and slumping in the direction parallel to the stopbank itself. Damage within the township of Blenheim was restricted to a small number of locations, and the impact on structures was low.

Significant damage occurred to a limited number of residential structures and two retaining walls in the town of Kaikoura, due to large ground movements which occurred in a concentrated zone within 30 m of Lyell Creek. Ejecta were not a common feature along the creek, and it is likely that soft silty/clayey materials in the upper soil profile are responsible for the movements. The wastewater treatment facility located just north of Kaikoura also suffered damage as a result of ground movements, which included tears in the liners of the oxidation ponds and distortions in the aeration system.

The impacts of liquefaction and general ground distress across the Amuri and Emu Plains of the Waiau Valley were extremely modest given the large peak accelerations observed in the area (i.e., horizontal accelerations of  $\approx 1$  g). The most significant impacts in this area were to the infrastructure where the high inertial loading caused structural damage to some of the bridges. Liquefaction and lateral spreading were observed at some bridge sites, but the impact and damage was generally secondary to those arising from the inertial loads. Characteristic damage to the bridges included settlement of the approach fills, outward cracking of the approach embankments, and some limited back-rotation of the bridge abutments.

No evidence of liquefaction was observed at four sites (located in Christchurch, Kaiapoi, and Waikuku Beach) where visible manifestation of liquefaction had occurred in many of the events of the 2010-2011 Canterbury Earthquake Sequence.

## References

- Arnold, T. (1847) *Letters from New Zealand and Tasmania, 1847–50*, p.83. ATL.
- ASTM (2007). “Standard Test Method for Particle-Size Analysis of Soils”. ASTM International, West Conshohocken, PA, 2011
- Begg, J. & Johnston, M. (2000). *Geology of the Wellington Area*. Lower Hutt, New Zealand: Institute of Geological and Nuclear Sciences 1:250 000 Map 10.
- Brown, L. (1981). Late Quaternary geology of the Wairau Plain, Marlborough, New Zealand. *New Zealand Journal of Geology and Geophysics*, 477-490.
- Cook, J. (1895) Map of Cloudy Bay survey district. Department of Lands and Survey
- Cowan, H.A. (1991). The North Canterbury earthquake of September 1, 1888, *Journal of the Royal Society of New Zealand*, **21**(1): 1-12.
- Cubrinovski, M., Green, R.A., Allen, J., Ashford, S., Bowman, E., Bradley, B.A., Cox, B., Hutchinson, T., Kavazanjian, E., Orense, R., Pender, M., Quigley, M., and Wotherspoon, L. (2010) Geotechnical reconnaissance of the 2010 Darfield (New Zealand) earthquake. *Bulletin of the New Zealand Society of Earthquake Engineering*. **43**(4): 243-321
- Cubrinovski, M., Bradley, B.A., Wotherspoon, L., Green, R.A., Bray, J.D., Wood, C., Pender, M., Allen, J., Bradshaw, A., Rix, G., Taylor, M., Robinson, K., Henderson, D., Giorgini, S., Ma, K., Winkley, A., Zupan, J., O’Rourke, T., DePascale, G., and Wells, D. (2011) Geotechnical aspects of the 22 February 2011 Christchurch Earthquake. *Bulletin of the New Zealand Society of Earthquake Engineering*. **44**(4): 205-226
- Hancox G.T., Perrin, N.D. & Dellow, G.D. (1997). *Earthquake-induced landslides in New Zealand and implications for MM intensity and seismic hazard assessment*. Institute of Geological & Nuclear Sciences Client Report 43601B (prepared for EQC).
- Litchfield, N.J., Benson, A., Bischoff, A., Hatem, A., Barrier, A., Nicol, A., Wandres, A., Lukovic, B., Hall, B., Gasston, C., Asher, C., Grimshaw, C., Madugo, C., Fenton, C., Hale, D., Barrell, D.J.A., Heron, D.W., Strong, D.T., Townsend, D.B., Nobe, D., Howarth, J.D., Pettinga, J., Kearse, J., Williams, J., Manousakis, J., Mountjoy, J., Rowland, J., Clark, K.J., Pedley, K., Sauer, K., Berryman, K.R., Hemphill-Haley, M., Stirling, M.W., Villeneuve, M., Cockroft, M., Khajavi, N., Barnes, P., Villamor, P., Carne, R., Langridge, R.M., Zinke, R., Vvan Dissen, R.J., McColl, S., Cox, S.C., Lawson, S., Little, T., Stahl, T., Cochran, U.A., Toy, V., Ries, W.F., and Juniper, Z. (2016). 14th November 2016 M7.8 Kaikoura Earthquake. Preliminary surface fault displacement measurements. Version 2. GNS Science. <http://dx.doi.org/10.21420/G2J01F>
- Marlborough Catchment Board (2017) *Wairau Valley Scheme*. Blenheim, Marlborough Catchment Board.

- Marlborough District Council (2016). Post-Kaikoura Earthquake Aerial Reconnaissance. Blenheim, Marlborough District Council.
- Marlborough District Council (2017). Smart Maps, <https://maps.marlborough.govt.nz/smartmaps>, Accessed 1 February 2017.
- Mason, D.P.M. & Little, T.A. (2006). Refined slip distribution and moment magnitude of the 1848 Marlborough earthquake, Awatere Fault, New Zealand. *New Zealand Journal of Geology and Geophysics*, 49, 375–382.
- Palermo, A., Liu, R., Rais, A., McHaffie, B., Andisheh, K., Pampanin, S., Gentile, R., Nuzzo, I., Granerio, M., Loporcaro, G., McGann, C. & Wotherspoon, L. (2017) Performance of road bridges during the 14<sup>th</sup> November 2016 Kaikoura Earthquake. *Bulletin of the New Zealand Society for Earthquake Engineering*. **50**(2): 253-270
- Robinson, K., Cubrinovski, M., Kailey, P. & Orense, R. (2011) “Field measurements of lateral spreading following the 2010 Darfield earthquake”. *Proceedings of the 9th Pacific Conference on Earthquake Engineering*, Auckland, New Zealand.
- Statistics NZ (2013) *Number of Electorates and Electoral Populations: 2013 Census*. Statistics NZ. ISBN 978-0-478-40854-6
- Thompson, A.S. (1859). *The story of New Zealand: past and present – savage and civilised*. Vol. 2. John Murray, London.
- Van Dissen, R.J. & Yeats, R.S. (1991). Hope fault, Jordan thrust, and uplift of the Seaward Kaikoura Range, New Zealand. *Geology*, **19**(4): 393-396.